# Testing the universality of the star formation efficiency in dense molecular gas

submitted to A&A

Y. SHIMAJIRI (CEA), Ph. André (CEA), J. Braine (Bordeaux Univ.), V. Könyves, S. Bontemps, (Bordeaux Univ.), N. Schneider (Cologne Univ.), B. Ladjelate, A. Roy, (CEA), Y. Gao (Chinese Academy of Science), H. Chen (Nanjing Univ.)





*STARFICH*

1. **Introduction**
   - + Filaments and Dense gas
   - + Universality of the relation between SFR and $M_{\rm dense}$
2. **Observations (IRAM, MOPRA, Nobeyama)**
3. **Results**
   - +Comparison among obtained maps
   - +Estimate of $M_{\rm dense}$
4. **Discussions**
   - +Variations in $\alpha_{\rm HCN}$
   - +Star Formation Rate in observed clouds
   - +Calibration of $M_{\rm dense}$ in external gal.
   - +Universality of relation between SFE and $M_{\rm dense}$
5. **Summary**
6. **南極望遠鏡による観測**

# Summary

Corrected $M_{dense}$ of extra gal.

based on our results of obs. toward nearby clouds.

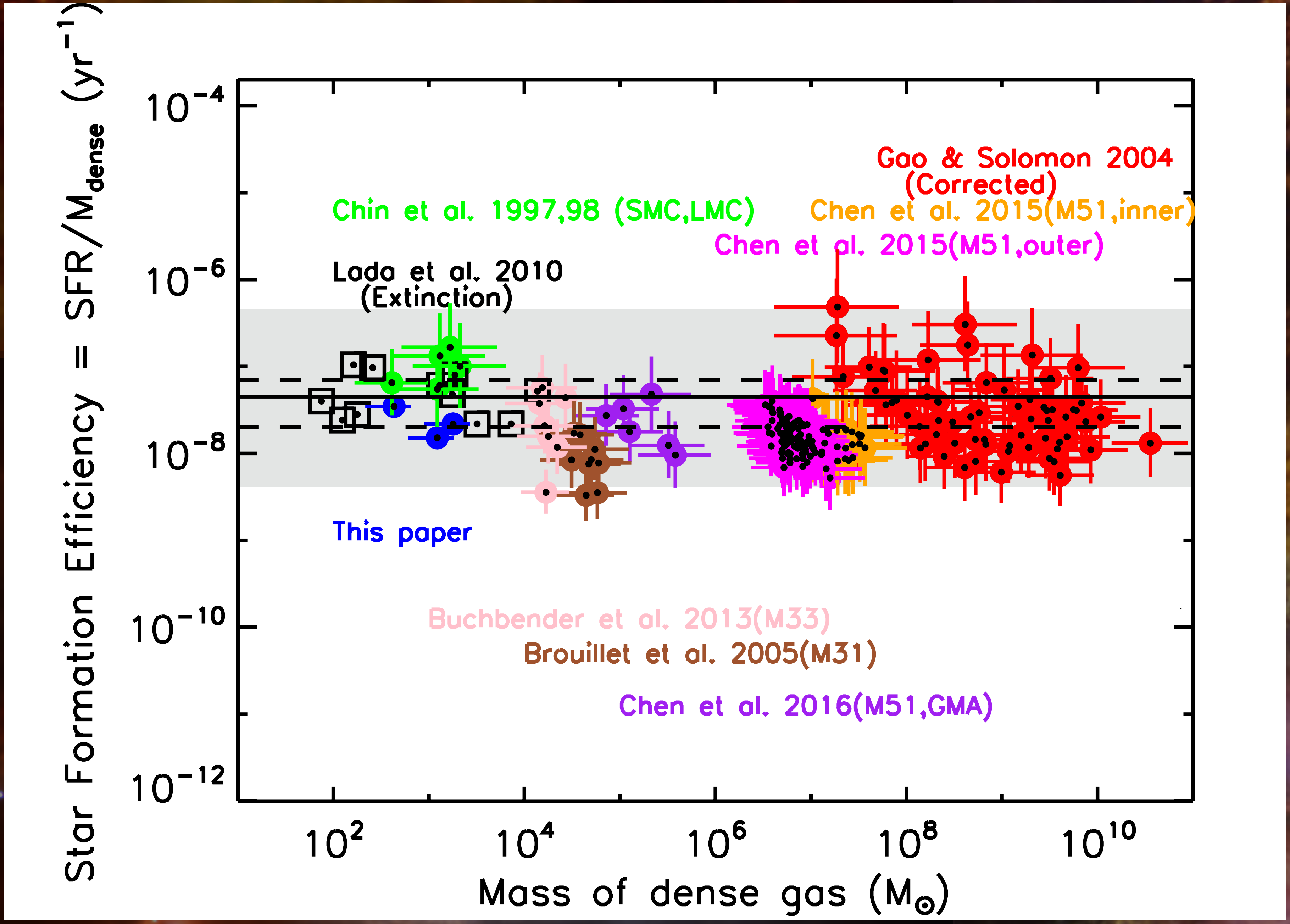


We found

constant SFE on a wide range of the scale from ~1-10pc to > 10 kpc

# Introduction:
# Herschel Gould Belt Survey Result

## Ubiquitous of filamentary structures in molecular clouds

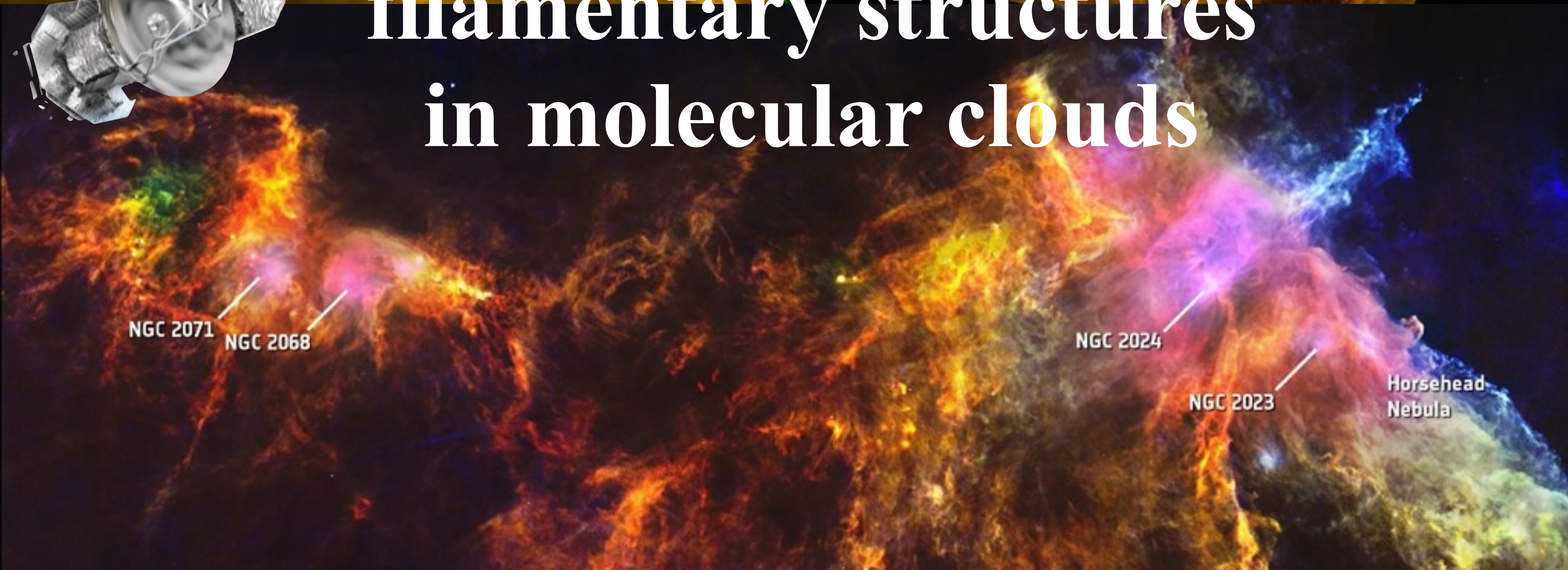


Andre et al. 2010, 2014, Molinari et al. 2010, Arzoumanian et al. 2011

# 0.1pc-width filaments

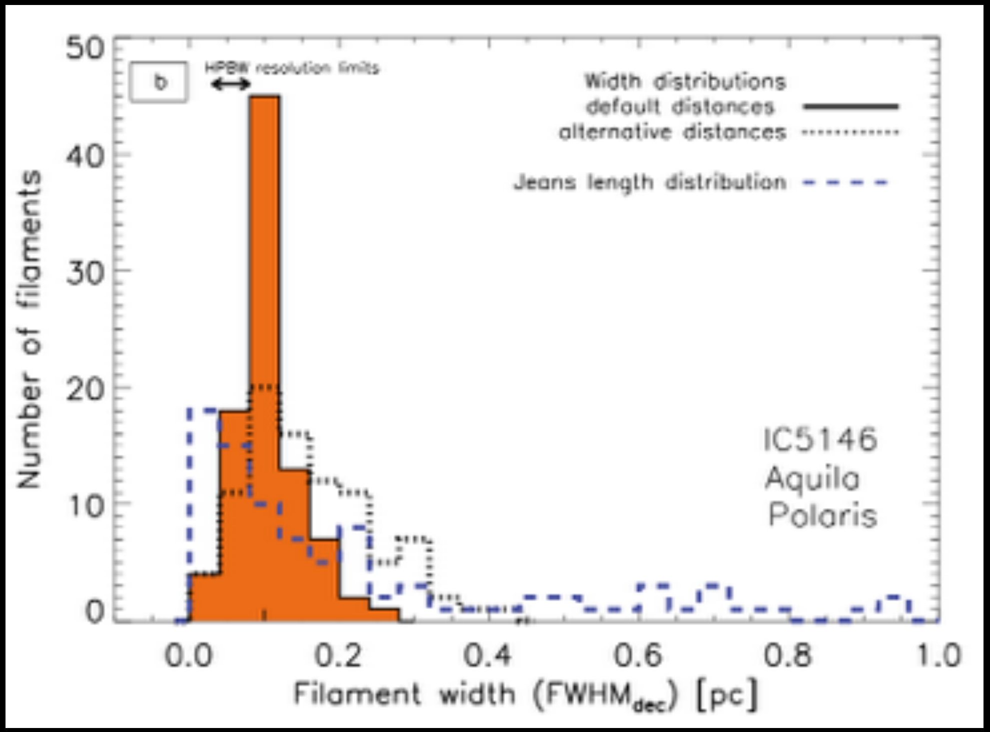


Arzoumanian+11

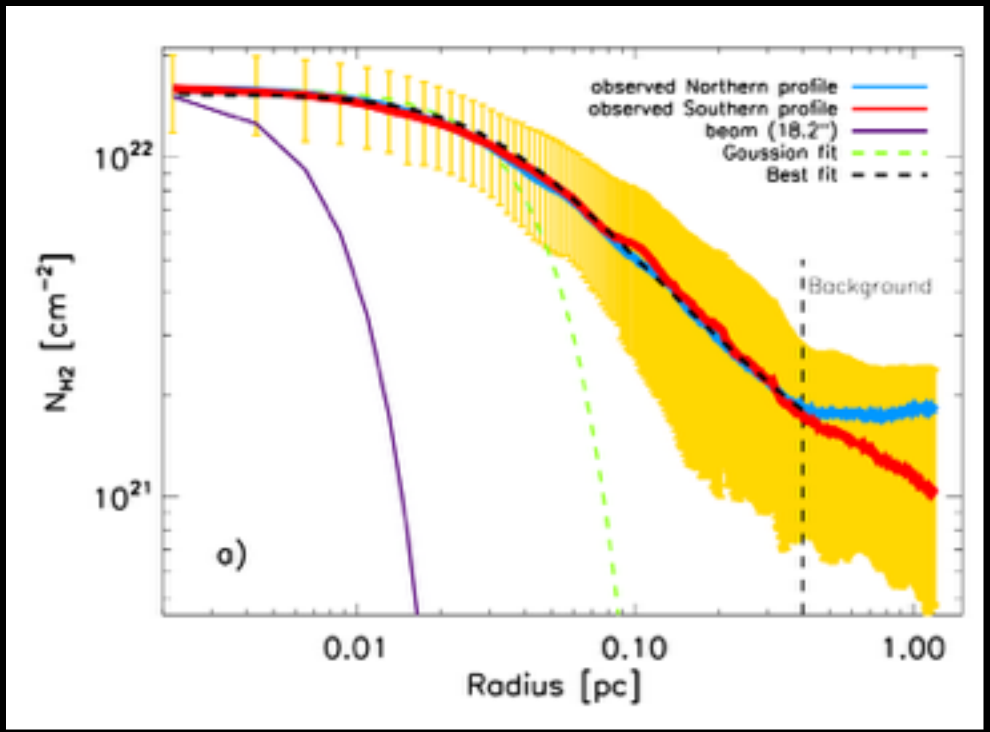


Palmeirim+13

# Structure inside filament

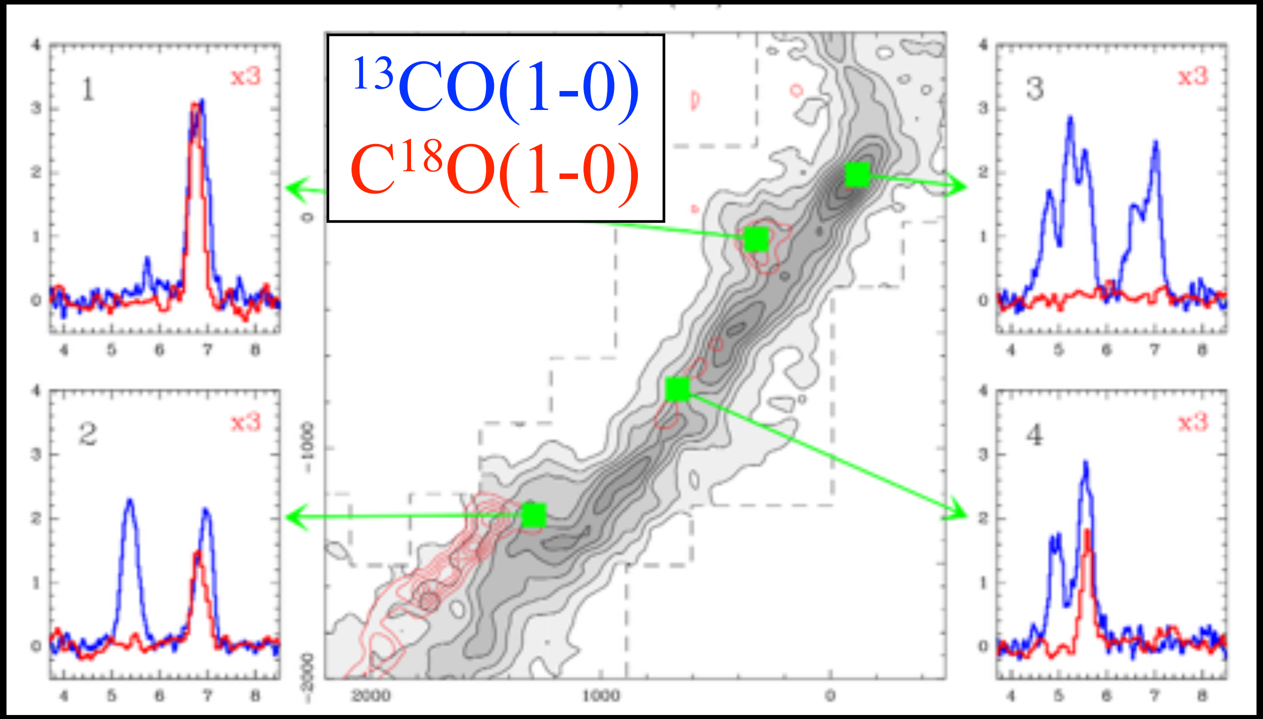


Hacar+13

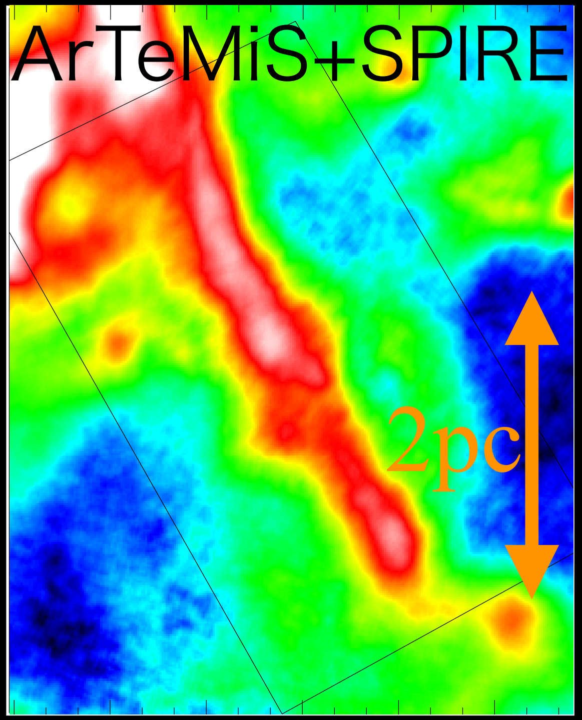


André et al. 2016

## 0.1pc-width filaments

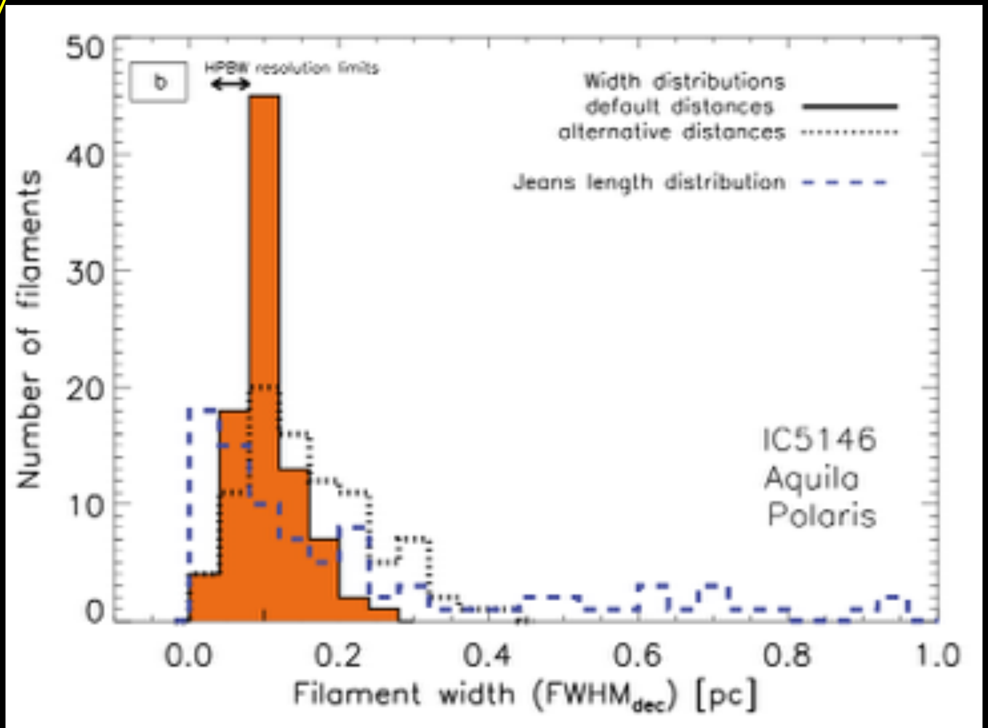


Arzoumanian+11

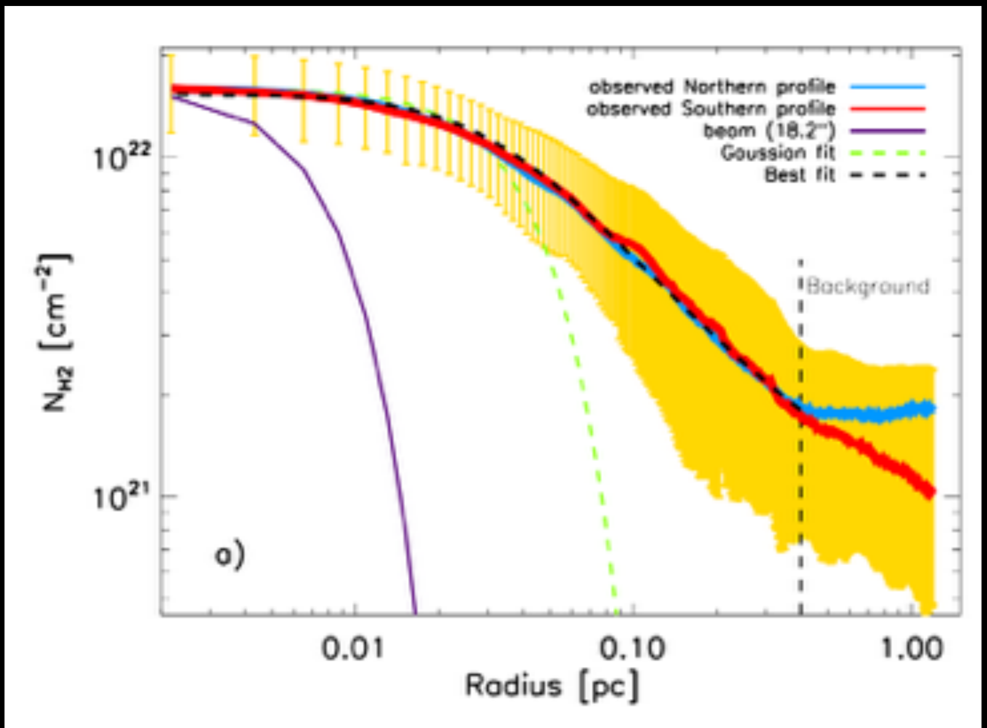


Palmeirim+13

## Structure inside filament

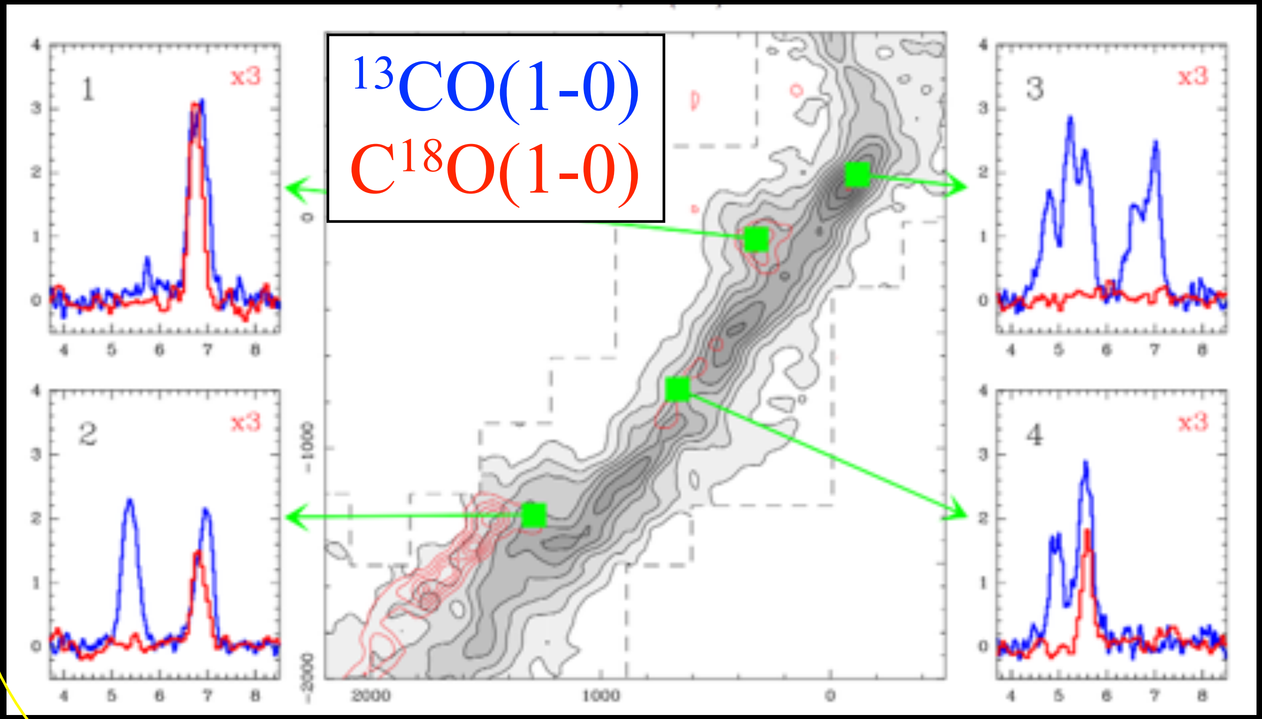


Hacar+13

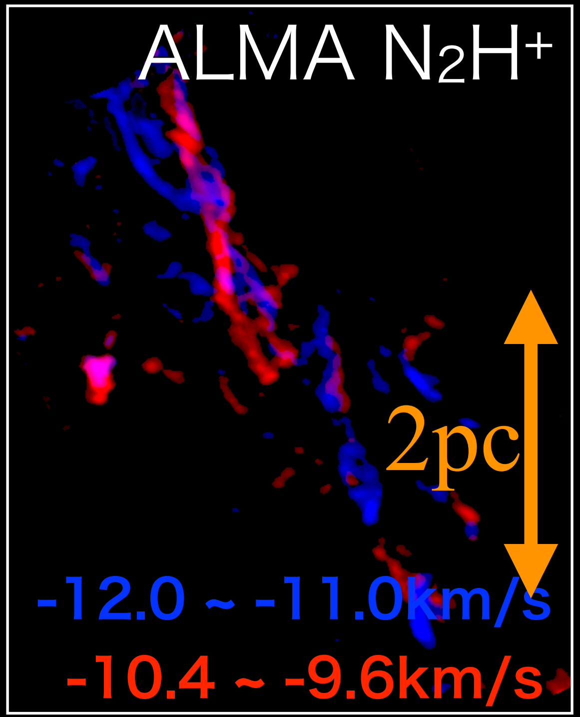


Shimajiri +in prep.

Give restrictions on theoretical filament studies

## Mass accretion

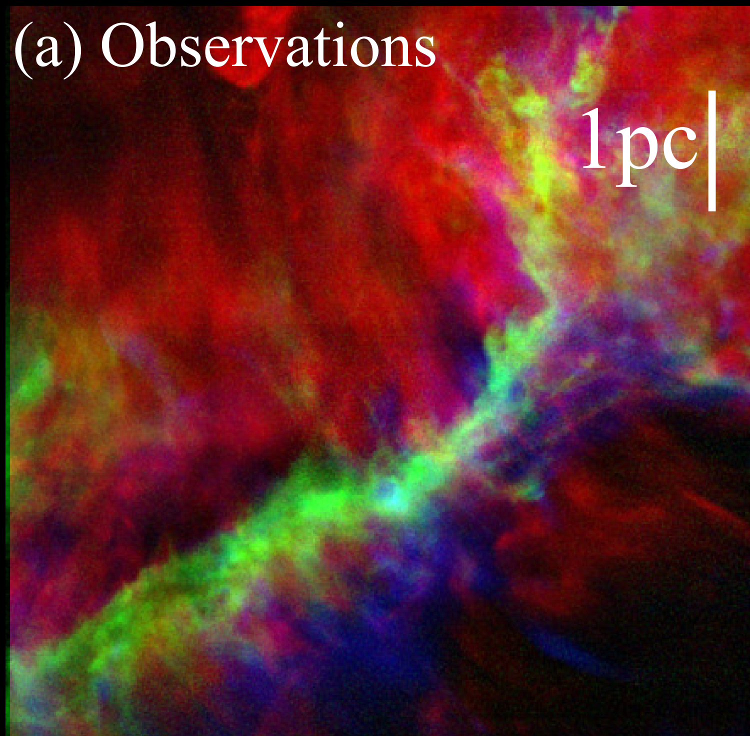


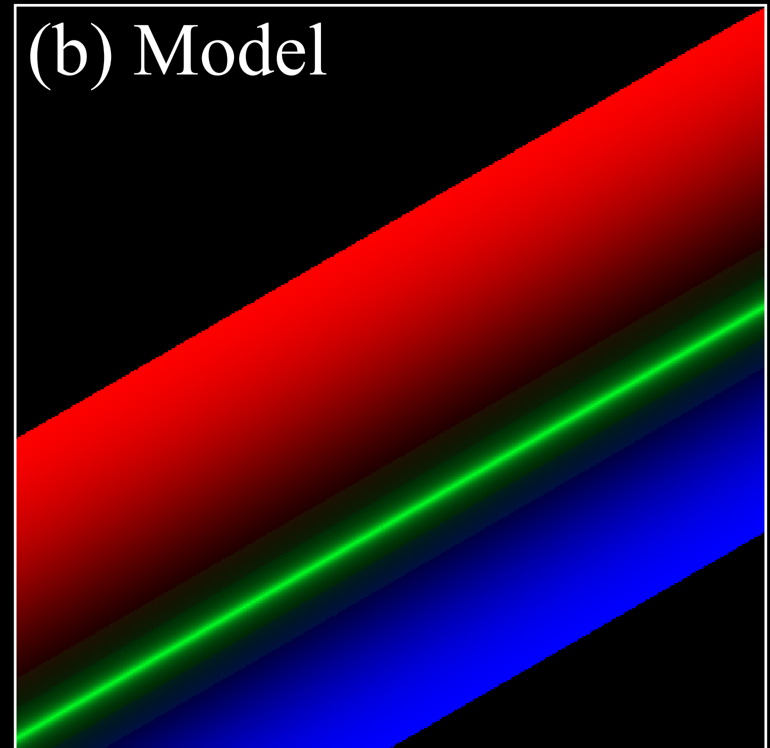


Palmeirim+13

Shimajiri+in prep.

$^{12}$CO(1-0):6.6-7.4km/s

$^{13}$CO(1-0):5.6-6.4km/s

$^{12}$CO(1-0):4.2-5.5km/s

**Accretion by gravity feeds filament.**

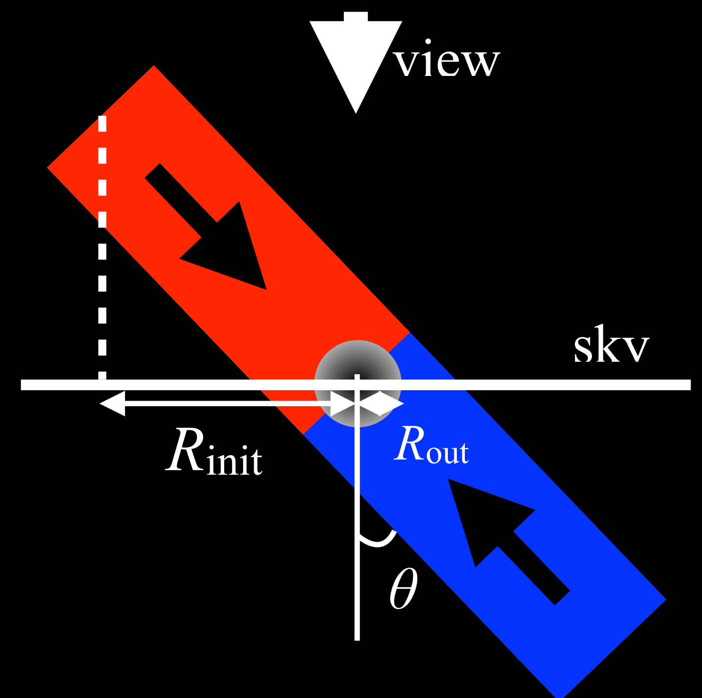


## Filaments to cores

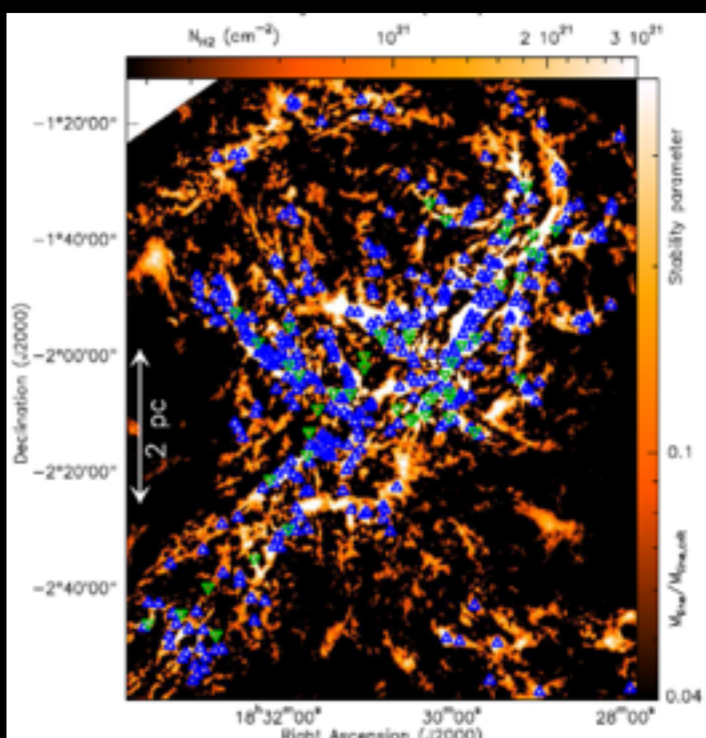

Konyves+15

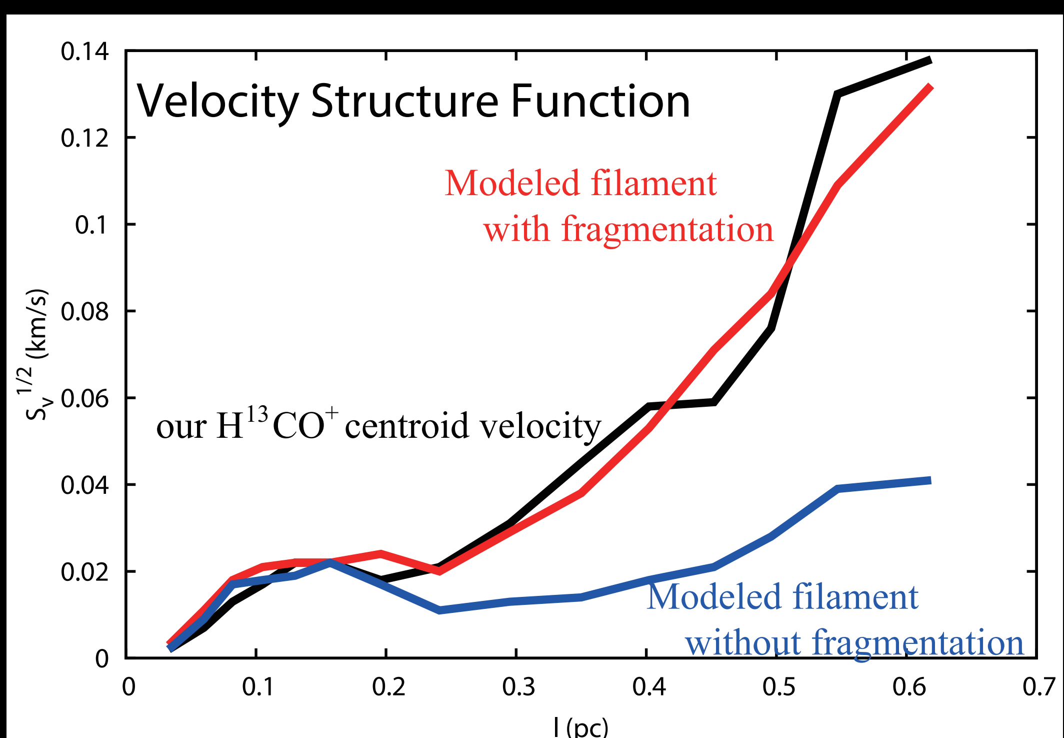


Shimajiri +in prep.

**Gravity causes fragmentation into cores**

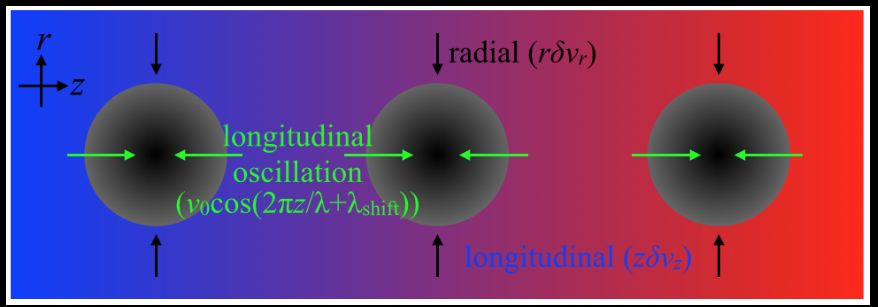

# Introduction:
# Mass budget in the Aquila cloud complex

## Column Density Probability Density Function

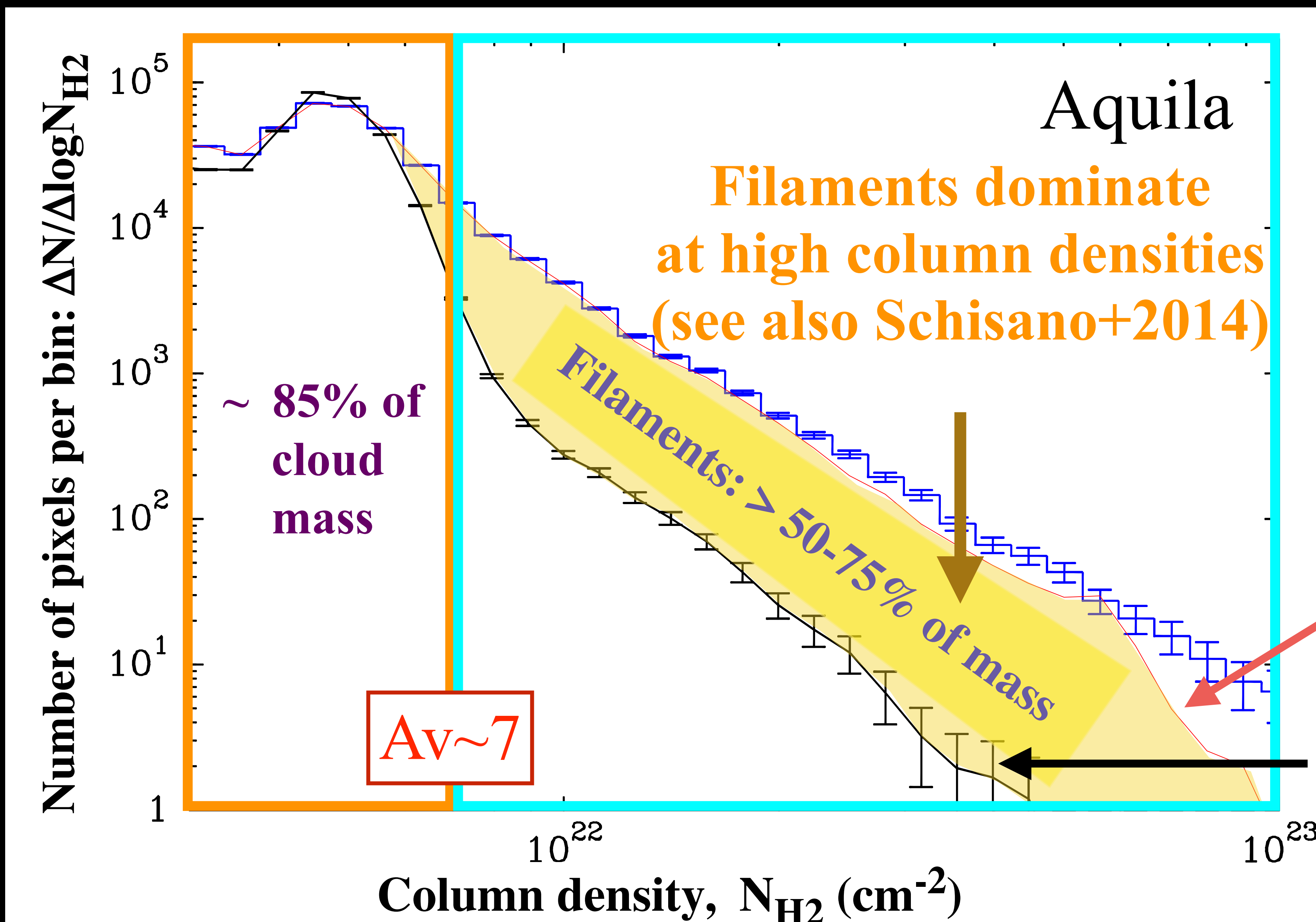


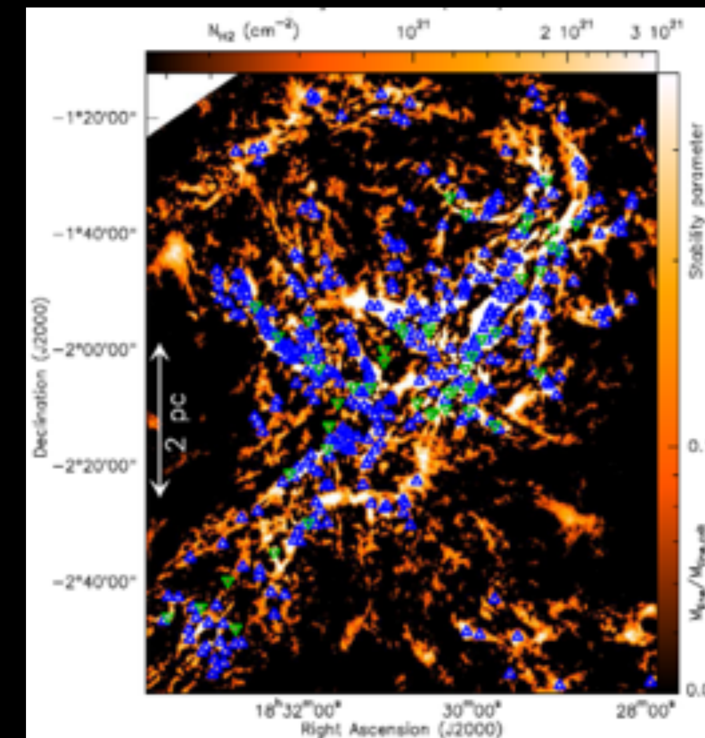


PDF
after subtracting cores

PDF
after subtracting cores & filaments
(Könyves et al. 2015)

- Below $A_V$ ~ 7: ~10-20% of the mass in the form in filaments,
  <1% in prestellar cores
- Above $A_V$ ~ 7: >50-75%of the mass in the form of filaments,
  $f_{pre}$~15±5% in prestellar cores

# Introduction: Density threshold for star formation

- ●Critical (thermal) mass per unit length: $M_{\rm line,crit}=2c_s^2/G$ (Stodolkiewicz 1963, Ostriker 1964)

- ●Thermally supercritical filament with $M_{\rm line} > M_{\rm line,crit}$: Unstable for radial collapse and gravitational fragmentation (Inustuka & Miyama 1992, 1997)

●$\boldsymbol{M_{\rm line,crit}} \sim$ **16 $\boldsymbol{M_{\rm sun}}$/pc @10K**

●$M_{\rm line,crit}/{\rm W_{fil}} \sim 160\ M_{\rm sun}/{\rm pc}^2$
which is corresponding to $A_{\rm V} \sim$ 8mag

●$M_{\rm line,crit}/W_{\rm fil}^2 \sim 1600\ {\rm M_{sun}/pc^3}$
which is corresponding to
$n({\rm H_2}) \sim 2.3\times10^{-4}\ {\rm cm}^{-3}$.

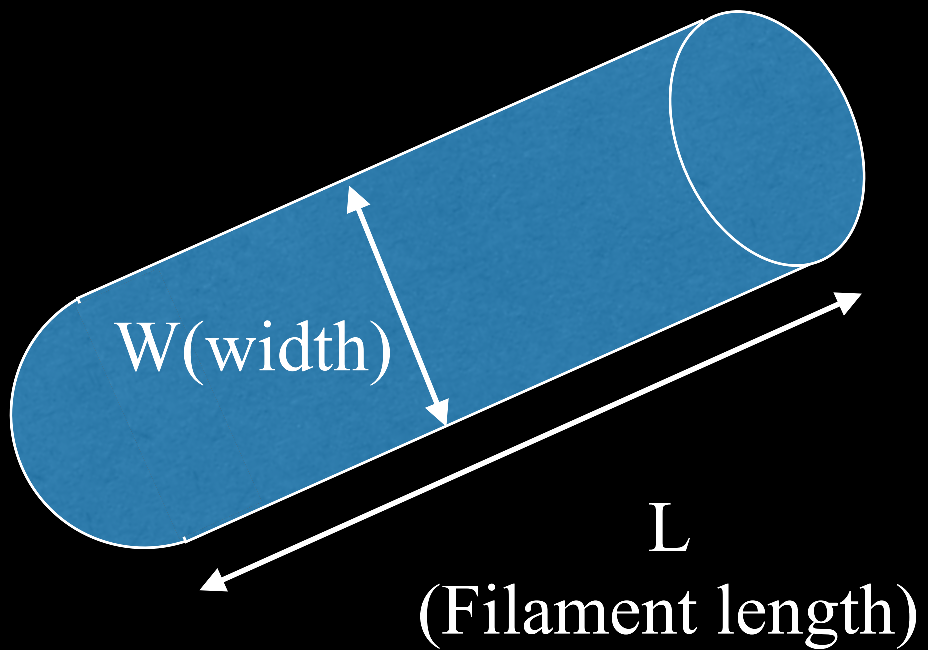


$M_{\rm line} = M\ /\ L$

# Introduction:
# Universality of the relation between SFR and $M_{dense}$

**SFR directly proportional to the mass of dense gas (≧$10^4$ cm$^{-3}$)**

SFR-$M_{dense}$ relation

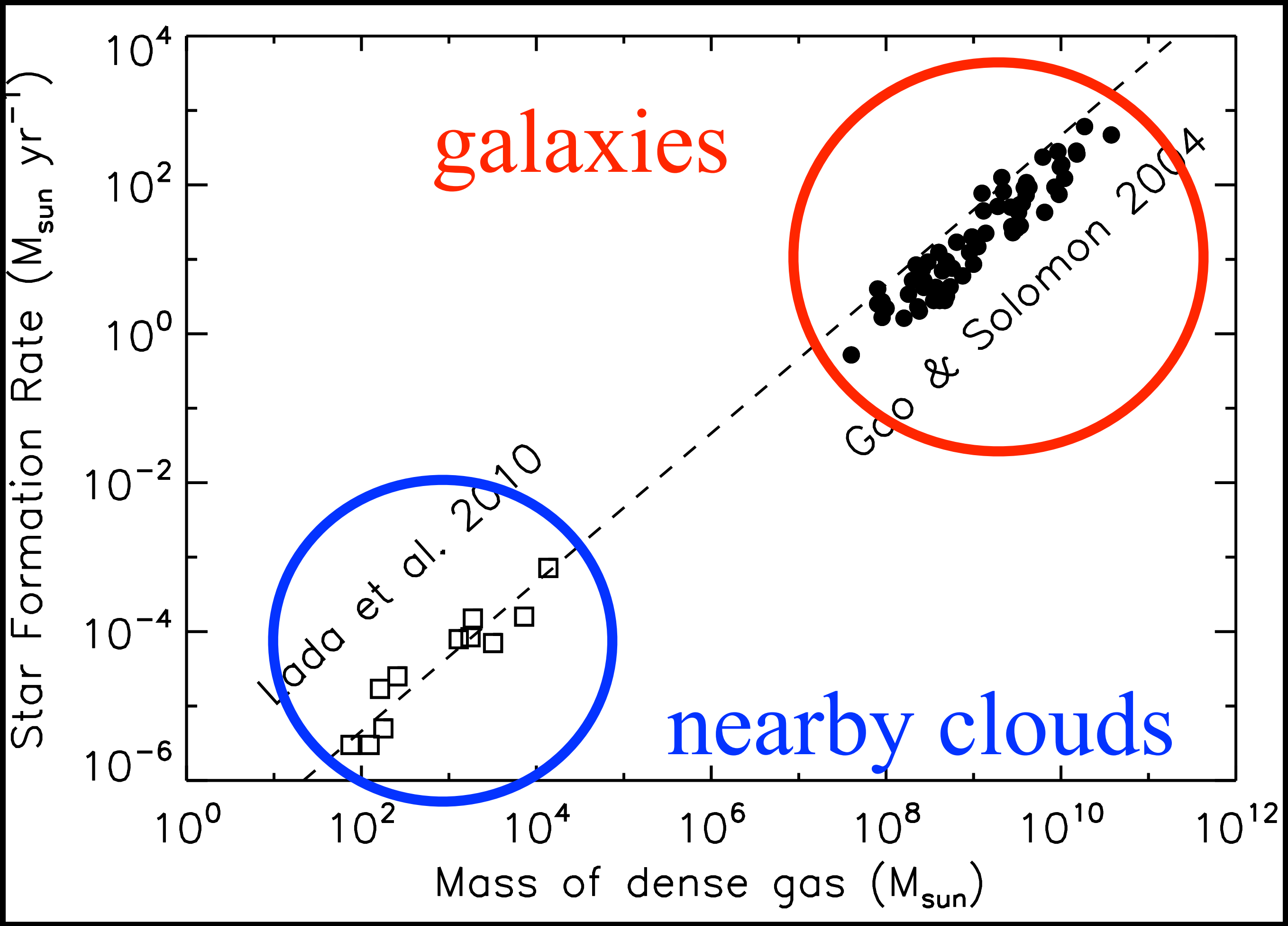


**[External galaxies]**

SFR=$1.8\times10^{-8}$ $M_{sun}$/yr × ($M_{dense}/M_{sun}$)
(Gao&Solomon 2004)

**[Nearby clouds]**

SFR=$4.6\times10^{-8}$ $M_{sun}$/yr × ($M_{dense}/M_{sun}$)
(Lada et al. 2010,12)

(also see Andre et al. 2014)

**The similar SFR-$M_{dense}$ relation has been found in the nearby galactic clouds and external galaxies.**

**May be a universal "star formation law" converting the dense gas into stars**

**$M_{dense}$ in external galaxies are larger than $M_{dense}$ expected from the SFR-$M_{dense}$ relation in the nearby clouds.**

# Introduction: Universality of the relation between SFR and $M_{dense}$

**SFR directly proportional to the mass of dense gas (≧$10^4$ cm$^{-3}$)**

SFR-$M_{dense}$ relation

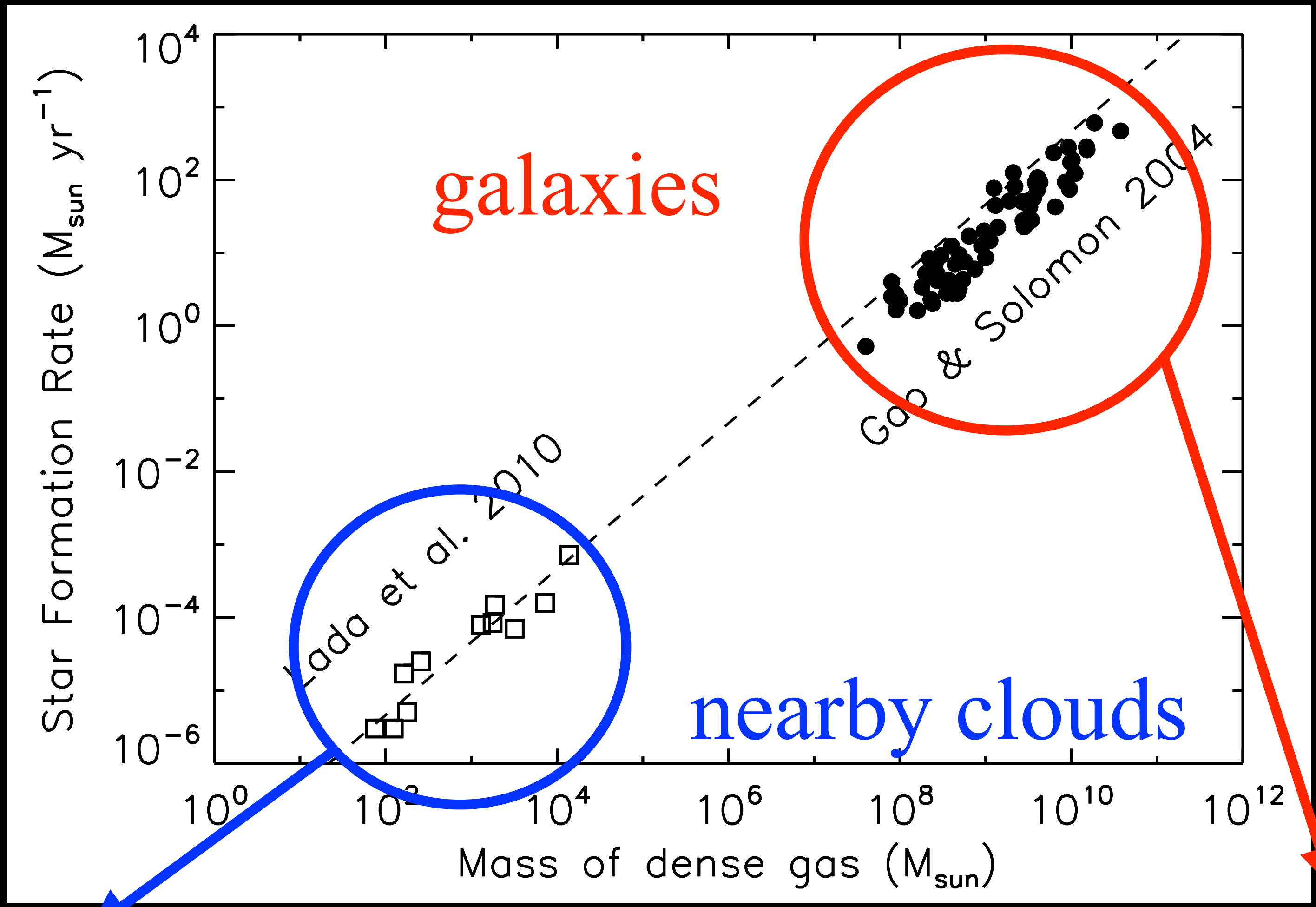


extinction

$M_{dense} = \alpha_{HCN} \times L_{HCN}$

*$\alpha_{HCN} = 10$

Different tracers were used to estimate $M_{dense}$.

→Observations in the same tracer are required.

# Introduction:
# Selection of molecular lines

$M_{\mathrm{line,crit}} \sim 16 M_{\mathrm{sun}}$/pc — n=$2.3\times10^{4}$ cm$^{-3}$

Effective excitation densities at 10K (Shirley 2015)

*Density results in a spectral line with 1 K km/s.

- HCN(1-0) — $8.4\times10^{3}$ cm$^{-3}$
- $H^{13}CN$(1-0) — $3.5\times10^{5}$ cm$^{-3}$
- $HCO^{+}$(1-0) — $9.5\times10^{2}$ cm$^{-3}$
- $H^{13}CO^{+}$(1-0) — $3.9\times10^{4}$ cm$^{-3}$

- ●Detectable in extra gal.
- ●Many HCN studies in extra gal.
  - ■Chin et al. 1997 (LMC)
  - ■Chin et al. 1998 (SMC)
  - ■Gao & Solomon 2004 (LIGs, ULIGs)
  - ■Brouillet et al. 2005 (M31)
  - ■Buchbender et al. 2013 (M33)
  - ■Chen et al. 2015, 2016 (M51)
  - etc…

# Molecular line observations

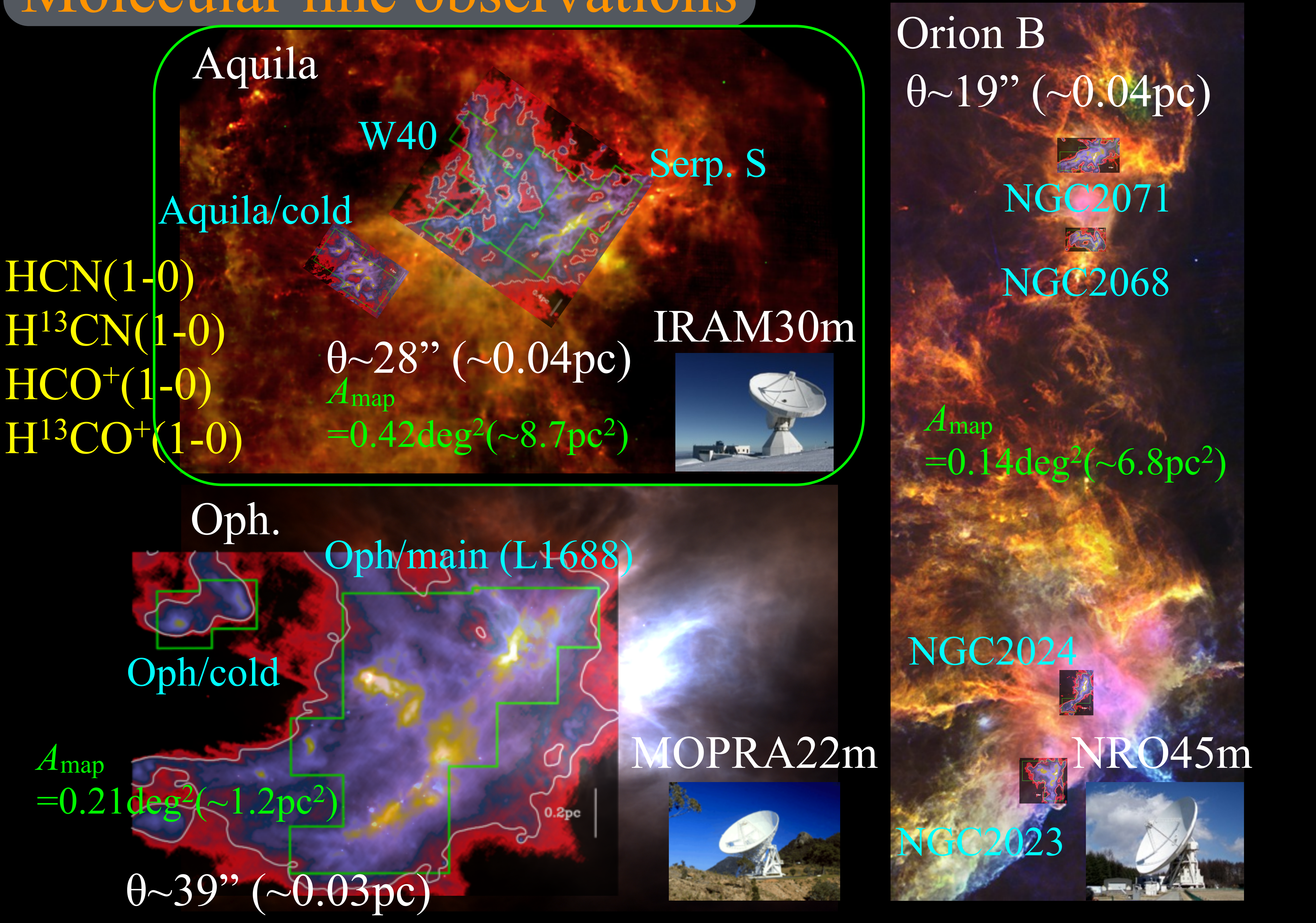

# Results: Maps in Aquila

Herschel $N(H_2)$

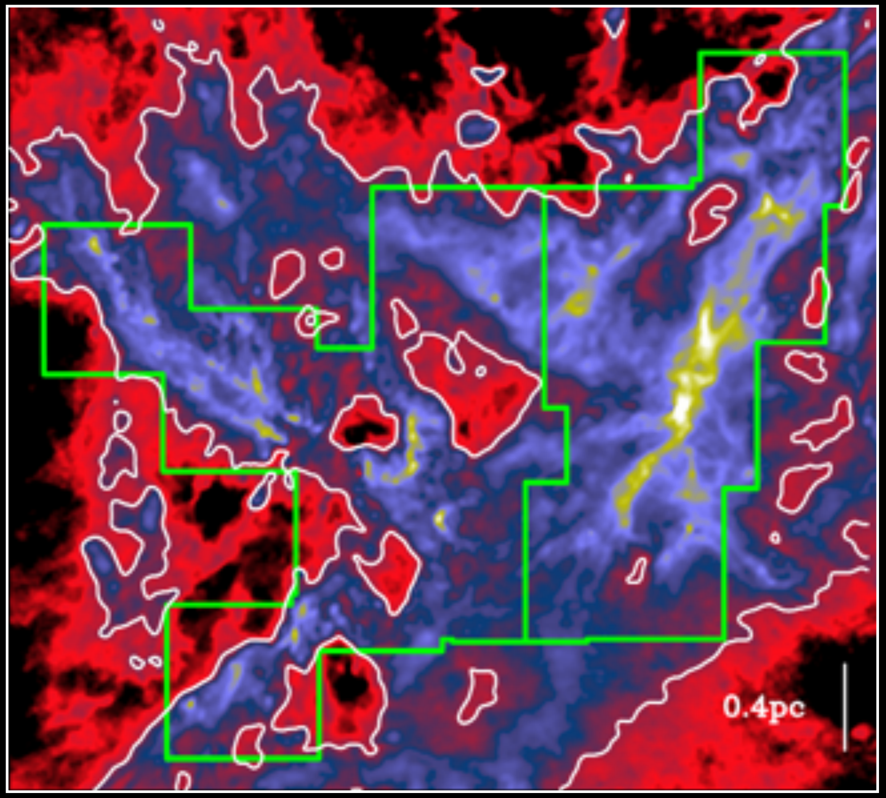


$H^{13}CO^+(1\text{-}0)$

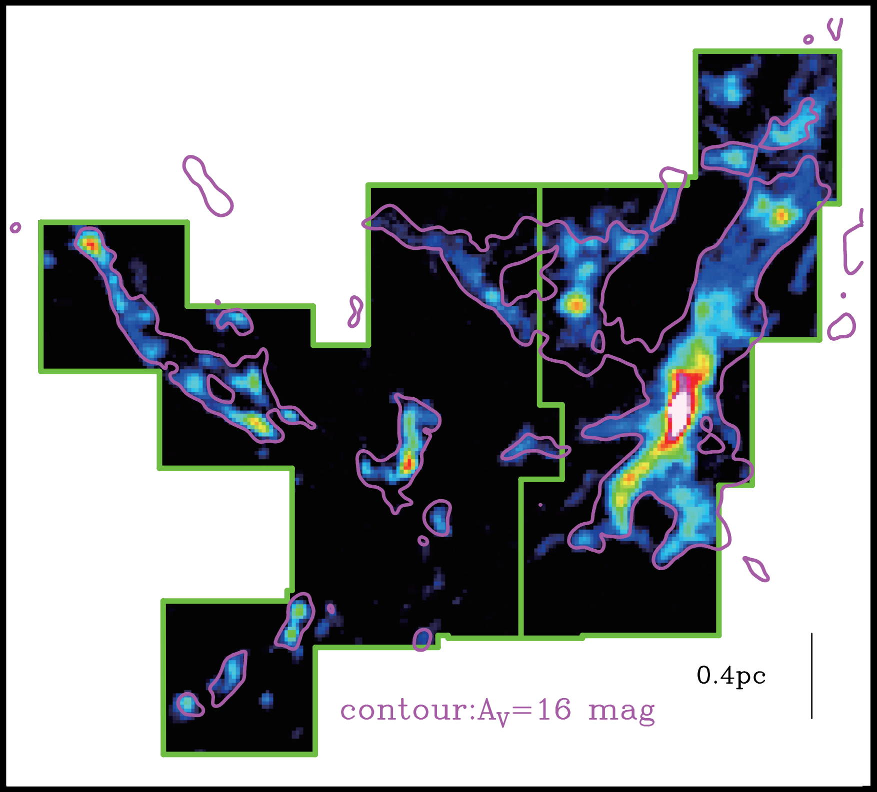


$H^{13}CN(1\text{-}0)$

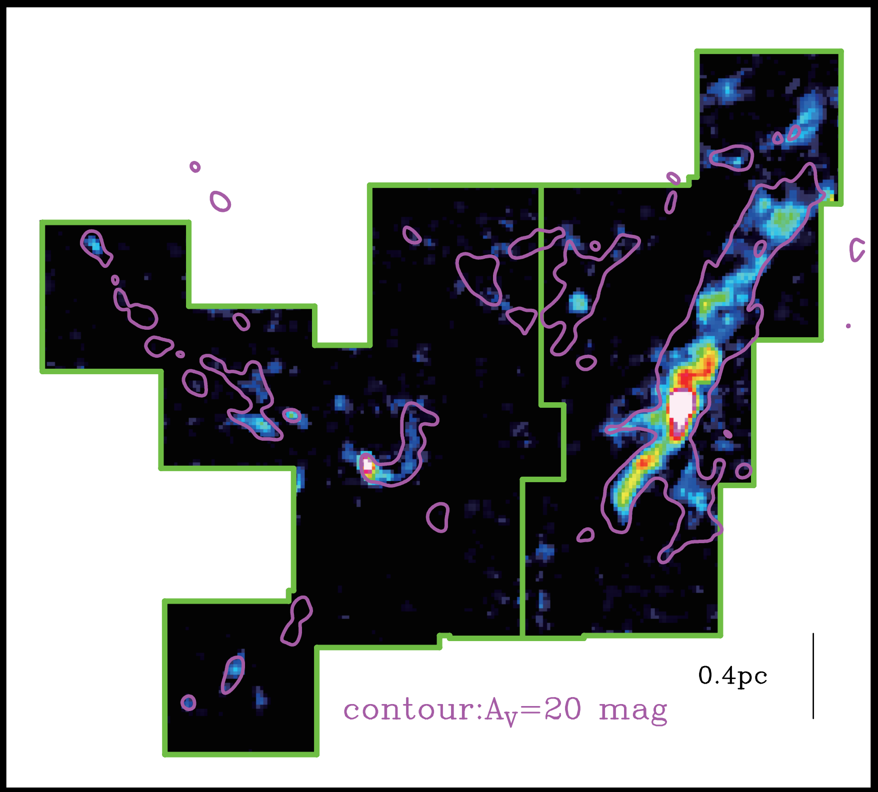


Distributions of $H^{13}CO^+$ & $H^{13}CN$
are similar to that of *Herschel* $N(H_2)$.

→Good tracers of "dense" Herschel filaments

# Results: Maps in Aquila

Herschel $N(H_2)$

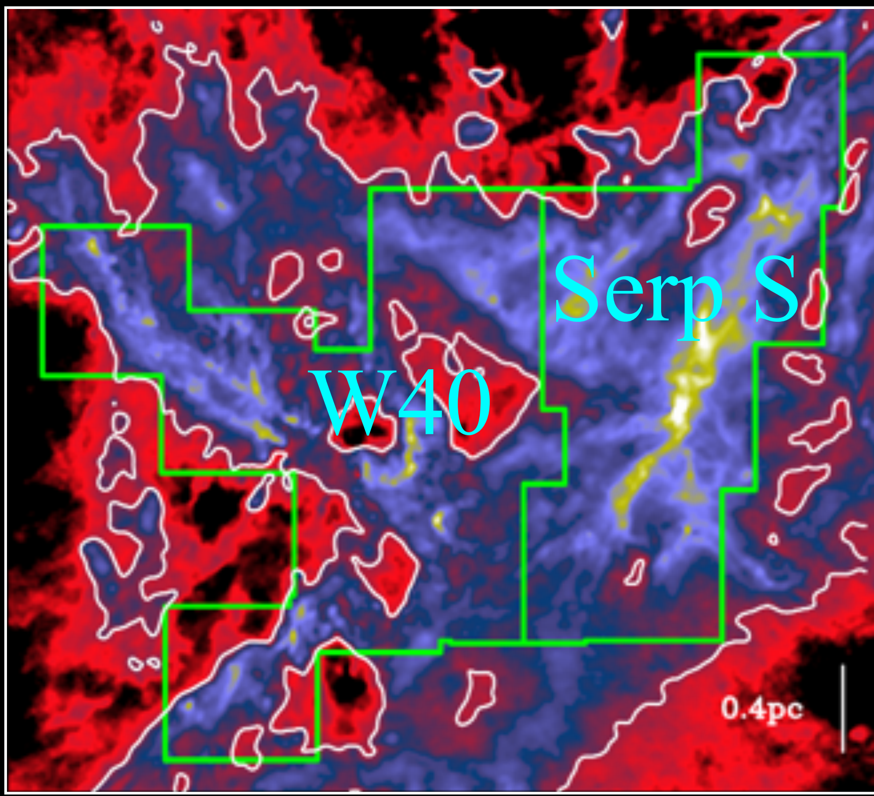


$HCO^+$(1-0)

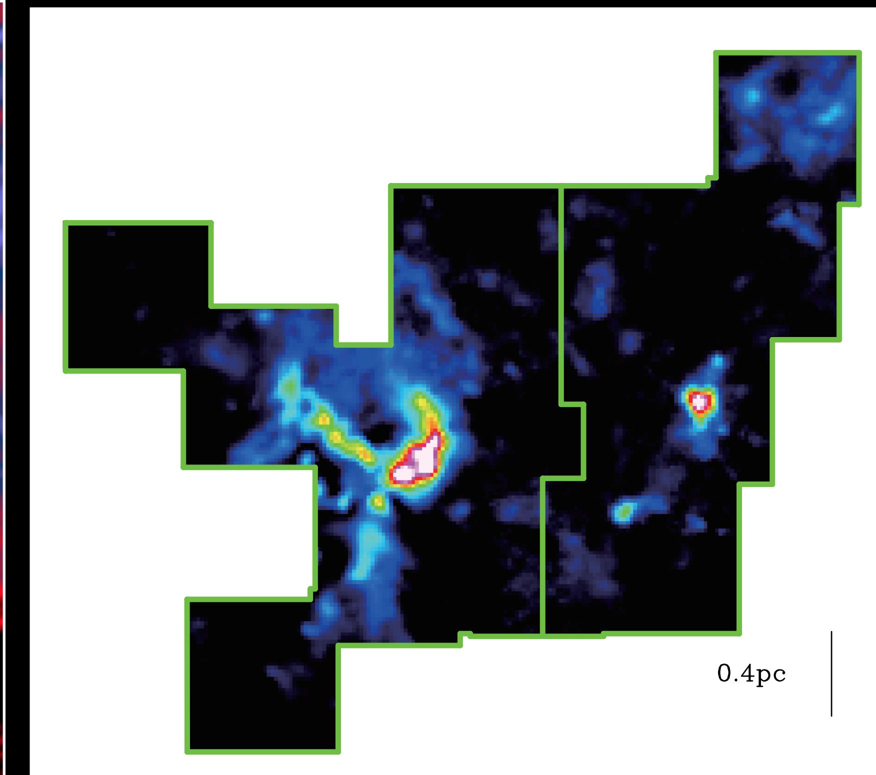


HCN(1-0)

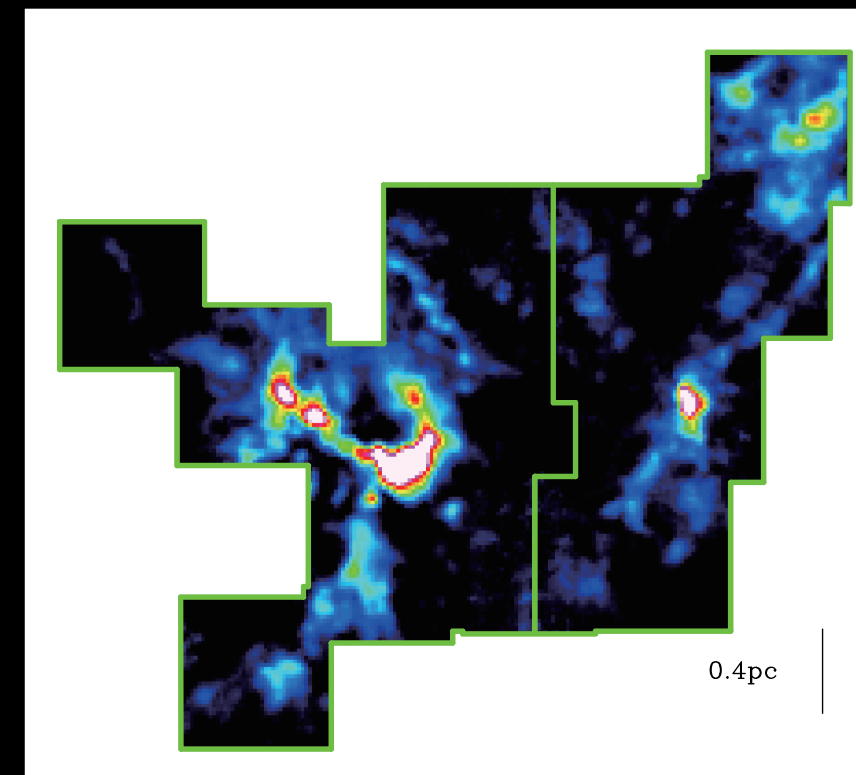


FUV field strength

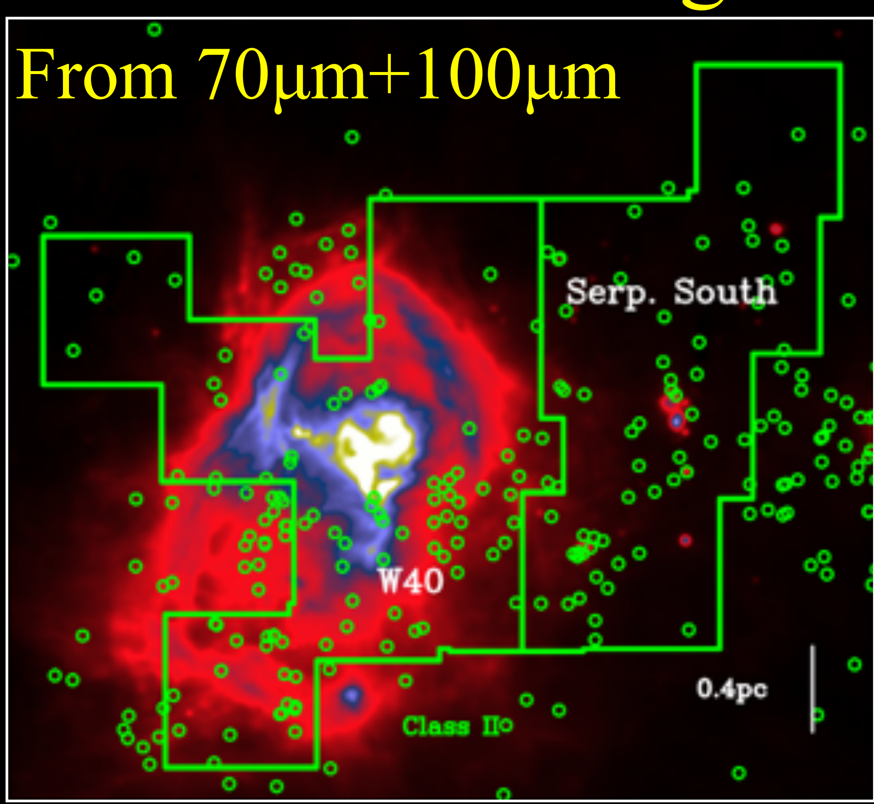


Stronger $HCO^+$ & HCN
around HII region.

→ Dependence of HCO+ & HCN
on FUV radiation

PDR model also predicts this dependence
(Meijrink et al. 2007)

# Discussion: Variations in $\alpha_{HCN}$

**Estimate $\alpha_{Herschel\text{-}HCN}$ in our observed clouds as below:**

$$\alpha_{Herschel\text{-}HCN} = M_{Herschel}^{map>8mag} / L_{HCN}$$

- Range of $\alpha_{Herschel\text{-}HCN}$ : 50-3800
- Much larger than $\alpha_{Herschel\text{-}HCN}$ used in other studies (e.g. 10:Gao & Solomon, 7±2: Wu et al. 2005)
- Large variations are recognized

Possible reason:

+ **FUV radiation (correlation coefficient = -0.82 → strong correlation)**

$$\alpha_{Herschel\text{-}HCN} = M_{Herschel} / L_{HCN} = 496 \times G_0^{-0.24}$$

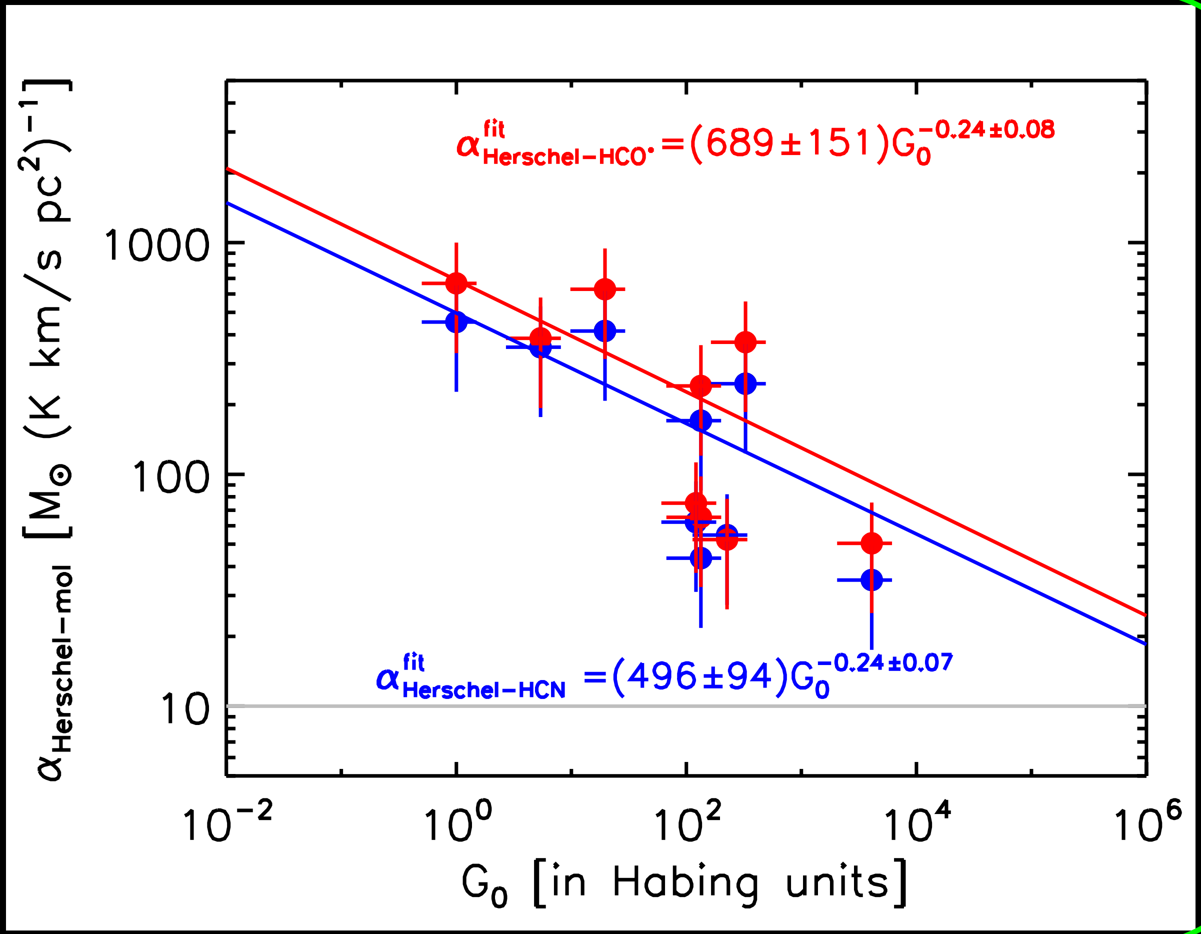

# Discussion: Star Formation Rate in observed clouds

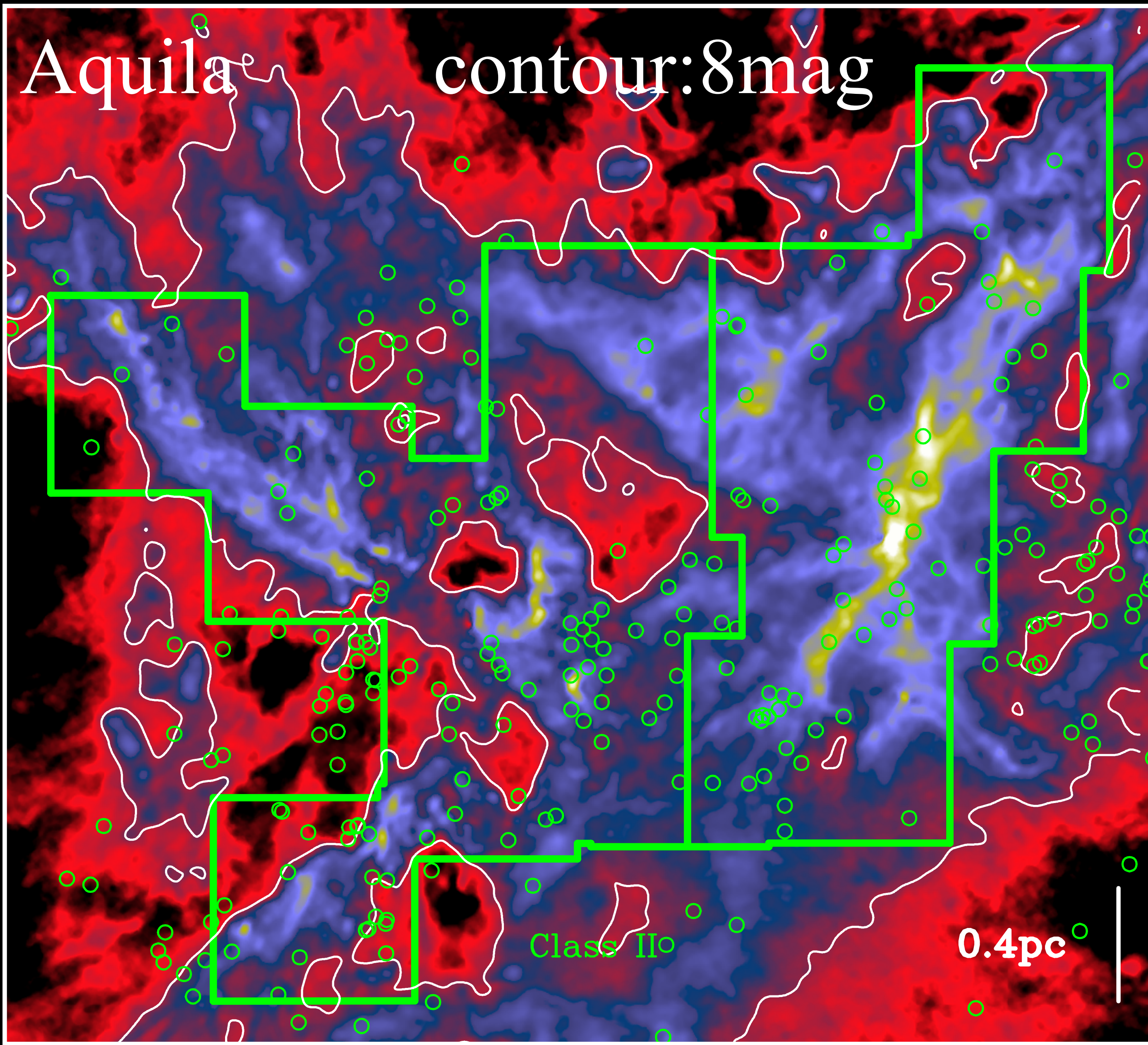


## Star formation rate (SFR)

$$\mathrm{SFR} = 0.25N(\mathrm{ClassII}) \times 10^{-6} M_{\odot}\mathrm{yr}^{-1}$$

Lifetime of Class II: 2 Myrs
Median mass : 0.5 $M_{\mathrm{sun}}$
(Covey+10, Dunham+15, Muench+07)

## Classification of protostars

**Class II: -1.6 ≦ α < -0.3**

(Greene et al. 1994)

## Spitzer YSO catalogs:

Dunham et al. 2015 for Oph and Aquila

Megeath et al. 2012 for Orion B

| | Oph (main) | Oph (cold) | W40 | Serp | Aquila (cold) | NGC2023 | NGC2024 | NGC2068 | NGC2071 |
|---|---|---|---|---|---|---|---|---|---|
| *N*(ClassII) | 59 | 0 | 54 | 54 | 7 | 8 | 29 | 4 | 20 |
| SFR (M | 14.8×10 | — | 13.5×10 | 13.5×10 | 1.8×10 | 2.0×10 | 9.0×10 | 1.0×10 | 5.0×10 |

# Discussion:
# Calibration of $M_{dense}$ in external gal.

## HCN survey toward etragal.

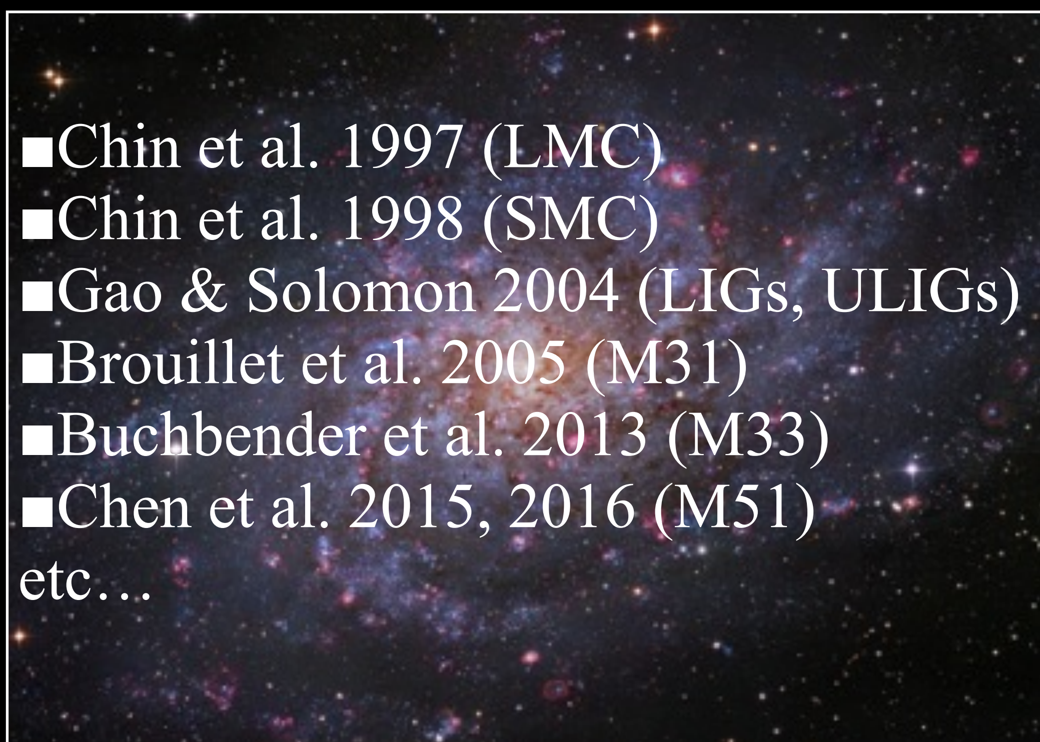


Beam size for external gal.
is much larger.
($\theta_{beam}$ = 9 pc — 36kpc)

HGBS $N(H_2)$

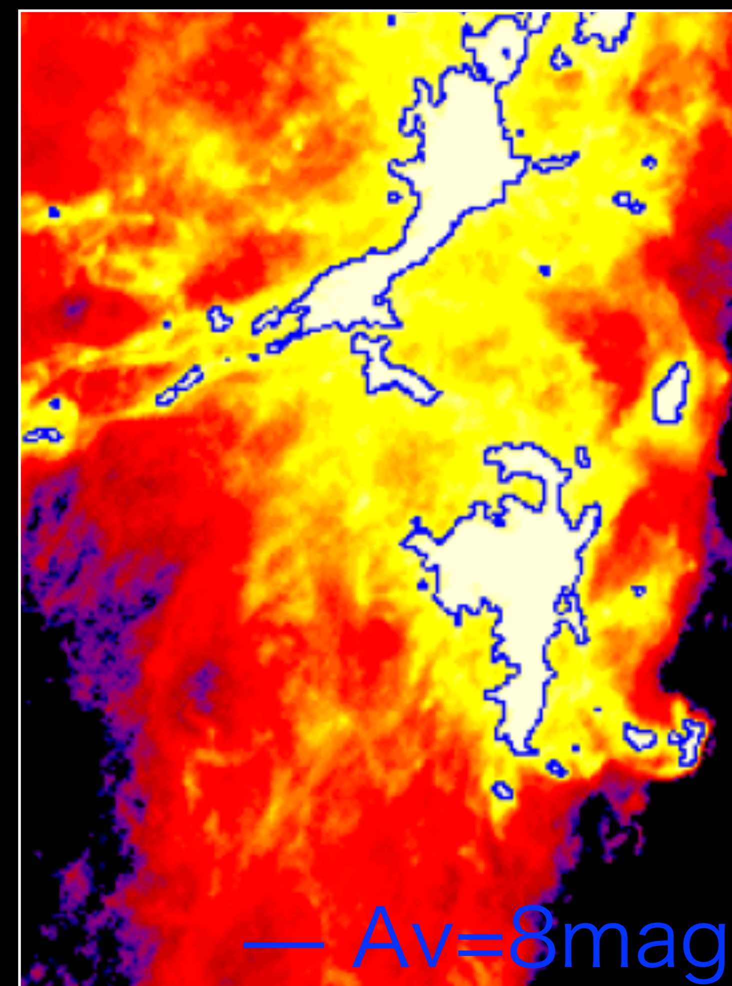


HCN(1-0)

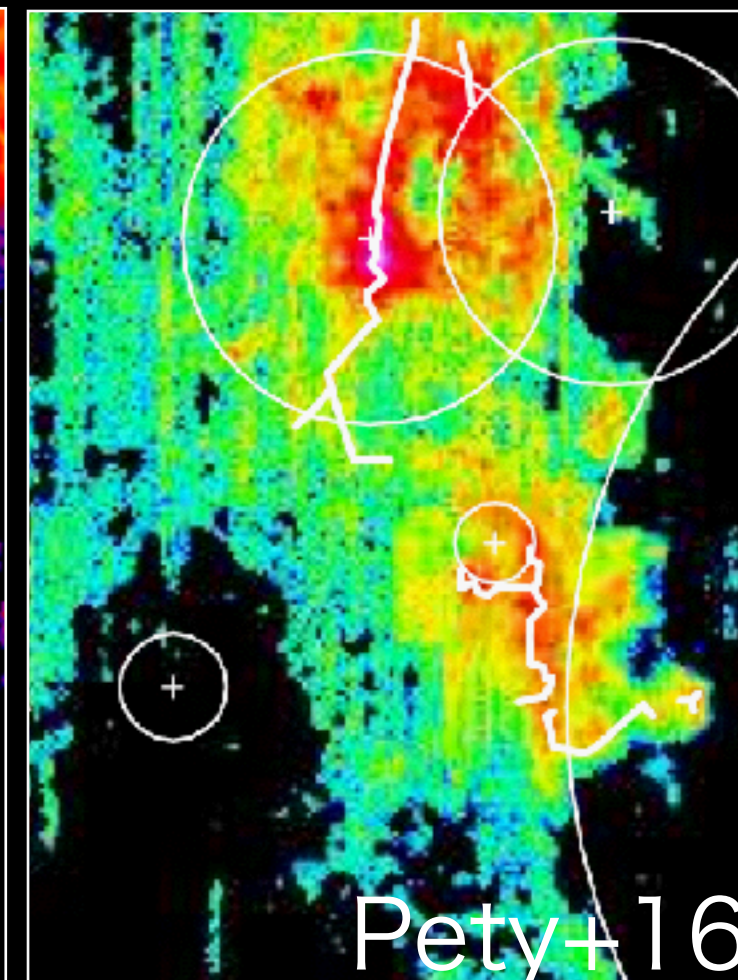


98% of HCN flux arises
from Av>2 area (Pety+16)

Need calibration of the contamination from lower *A*v area.

# Discussion: Calibration of $M_{dense}$ in external gal.

## Column Density Probability Density Function

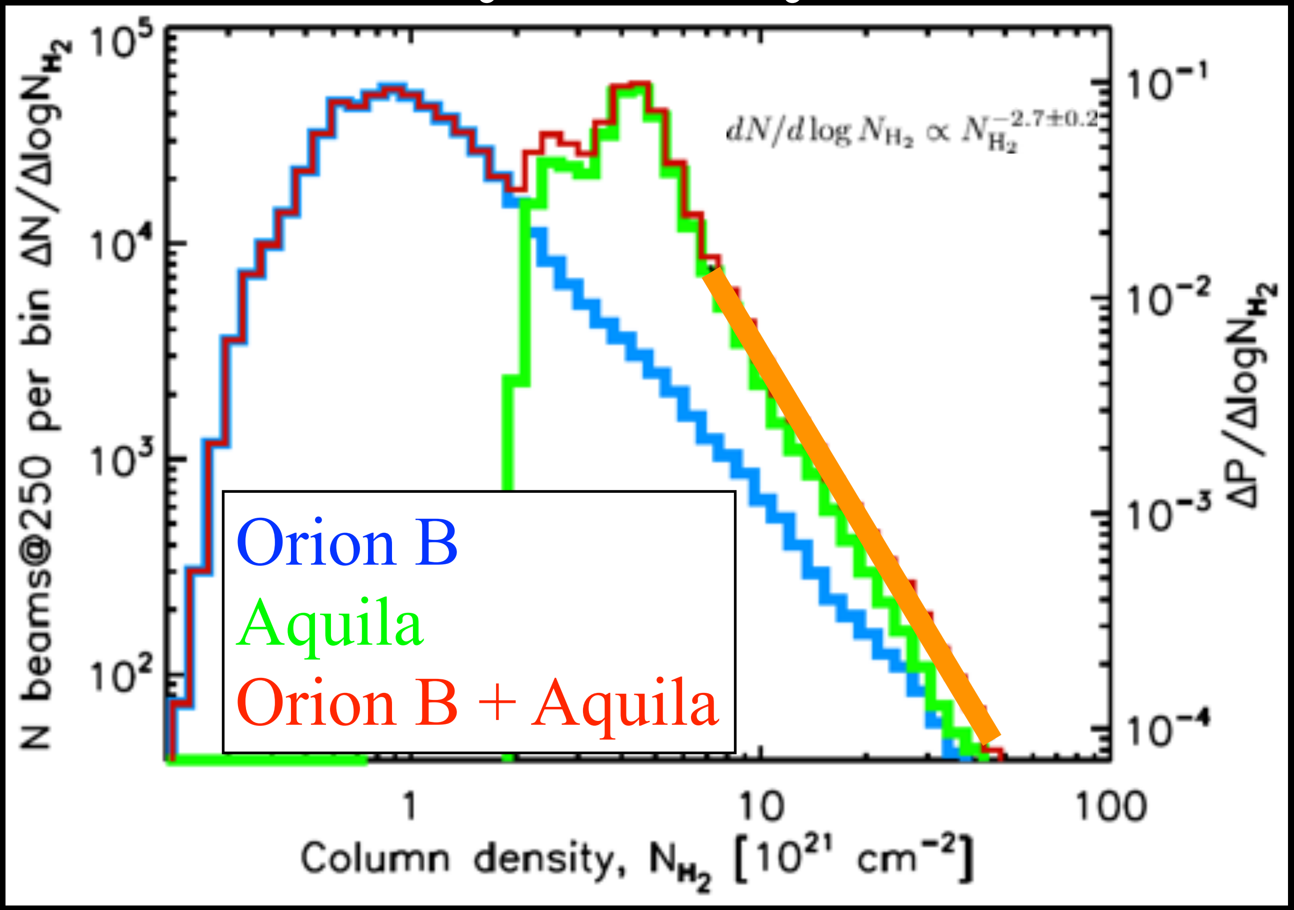


Könyves et al. 2015, Könyves et al. in prep.

## Dependence of effective excitation densities on Temperature

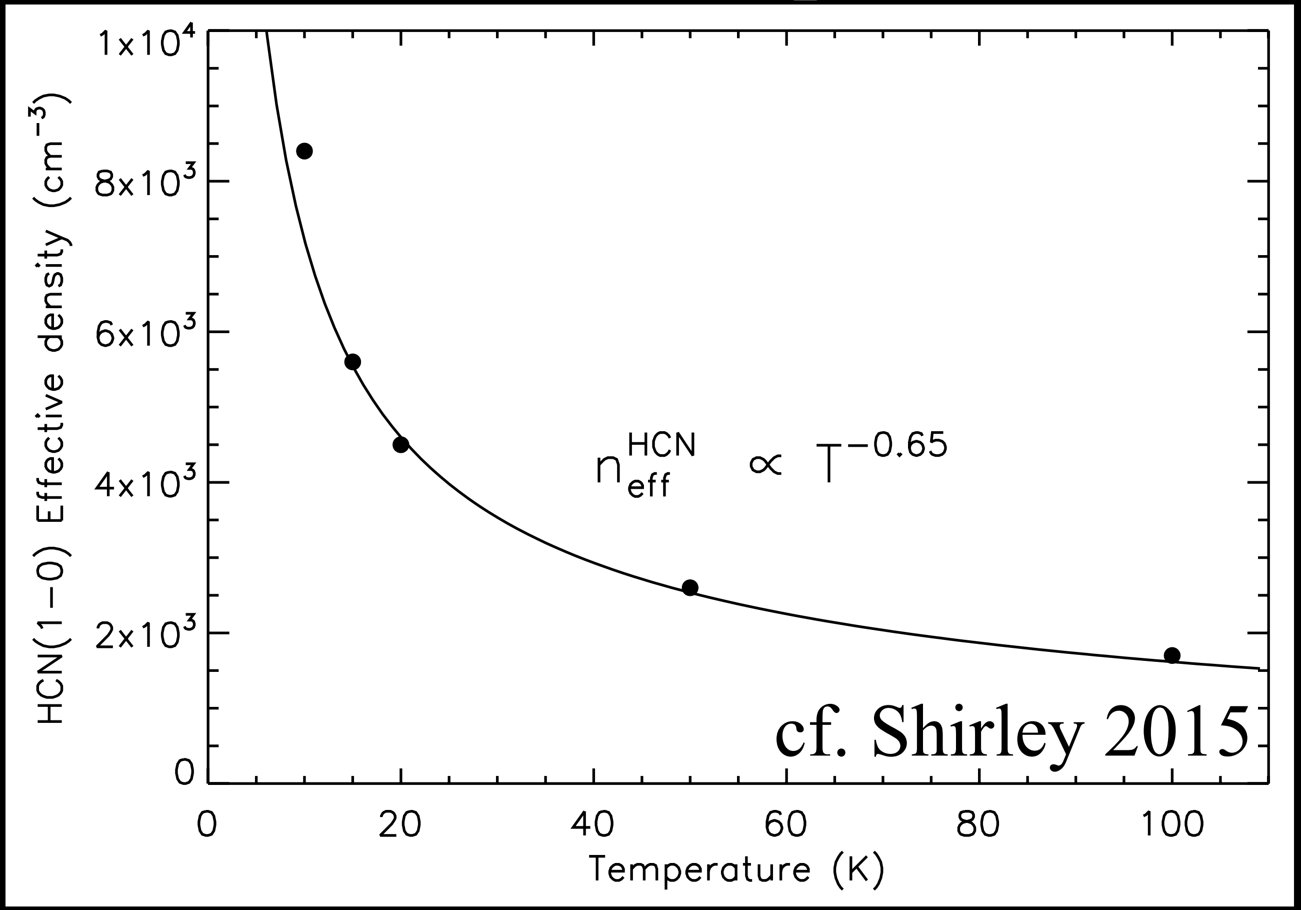


Assumptions:

$$T_{dust} \propto G_0^{0.2} \qquad N_{H_2} \propto \rho^{1-\frac{1}{\alpha}} \ (\alpha = 1.75 \pm 0.25)$$

$$\frac{M(A_V > 2\mathrm{mag})}{M(A_V > 8\mathrm{mag})} = \left(\frac{A_V = 2\mathrm{mag}}{A_V = 8\mathrm{mag}}\right)^{-1.7\pm0.2} \approx 10$$

$$L_{HCN,Av=2} \propto (n_{eff}^{HCN})^{0.43} \propto G_0^{0.056\pm0.012}$$

$$\alpha_{Herschel-HCN}^{fit'} \approx 0.13_{-0.06}^{+0.06} \times G_0^{-0.095\pm0.02} \times \alpha_{Herschel-HCN}^{fit} \propto G_0^{-0.34\pm0.08}$$

# Discussion:
# Relation between SFR and $M_{dense}$

Corrected SFR-$M_{dense}$ relation

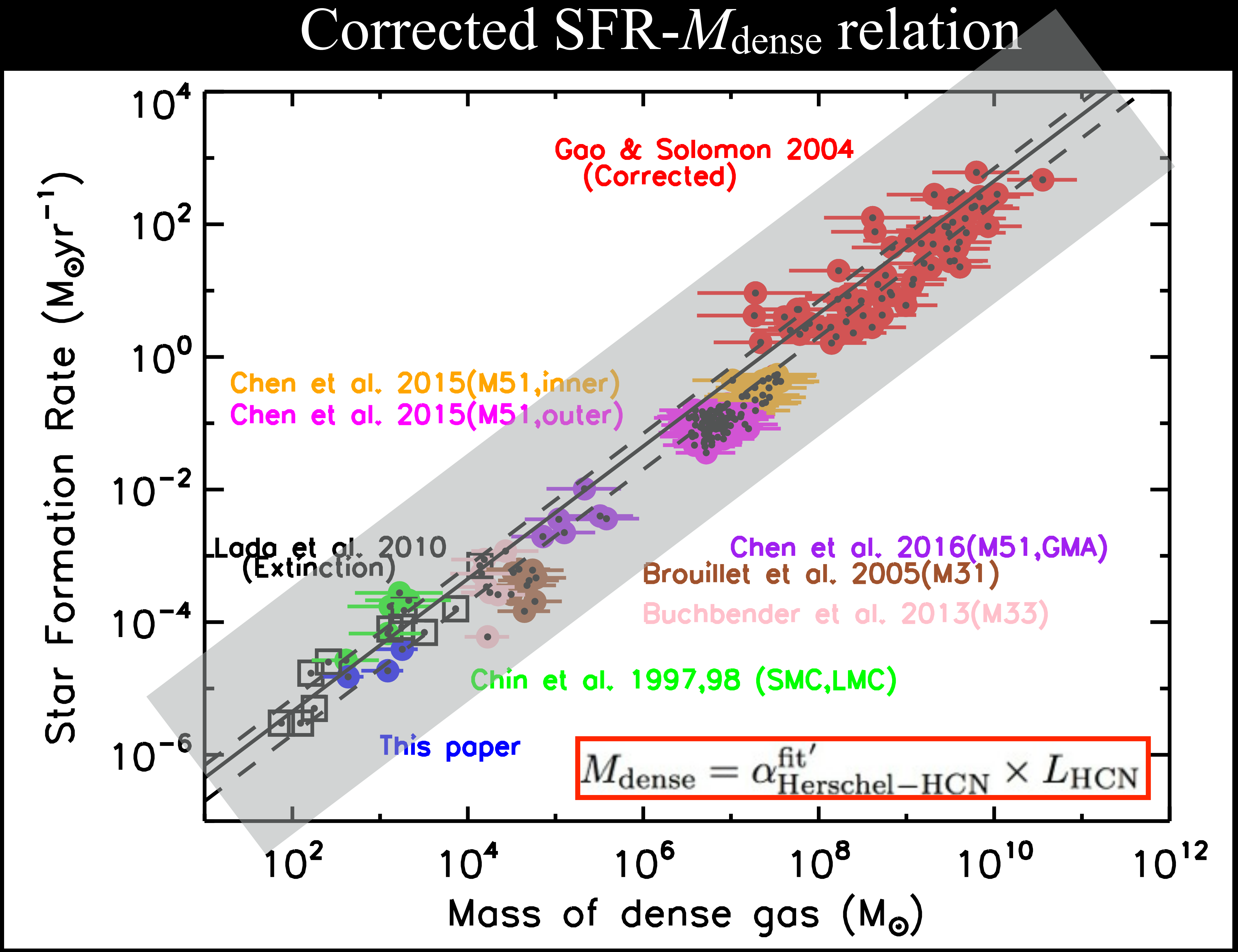


**Linear relation between SFR and $M_{dense}$**

# Discussion:
# Relation between SFE and $M_{\text{dense}}$

Corrected SFE-$M_{\text{dense}}$ relation

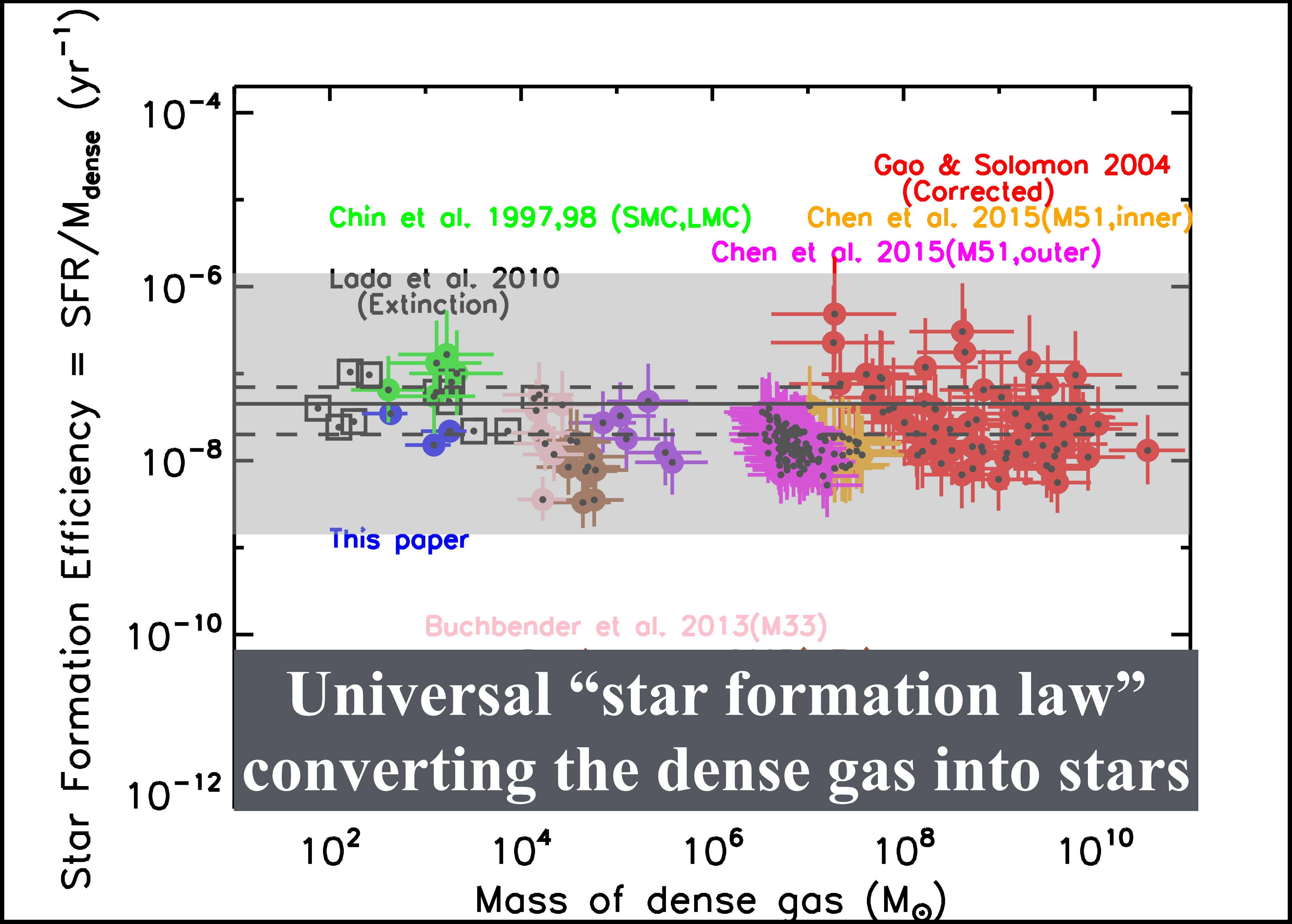


**Universal "star formation law" converting the dense gas into stars**

Constant SFE on a wide range of the scale from ~1-10pc to > 10 kpc

# Summary

- We conducted a wide field mapping in HCN, $HCO^+$, $H^{13}CN$, and $H^{13}CO^+$ toward Aquila, Oph., and Orion B.

- $H^{13}CO^+$ and $H^{13}CN$:
  **Good tracers of "dense" Herschel filaments.**

- Larger variations in $\alpha_{HCN}$ (=$M_{dense}/L_{HCN}$) conversion factor.
  → $\alpha_{HCN}$ decreases as $G_0$ increases ($\alpha_{HCN} \propto G_0^{-0.24}$).

- Corrected $M_{dense}$ for the external galaxies
  **Constant SFE on a wide range of the scale from ~1-10 pc to > 10 kpc.**

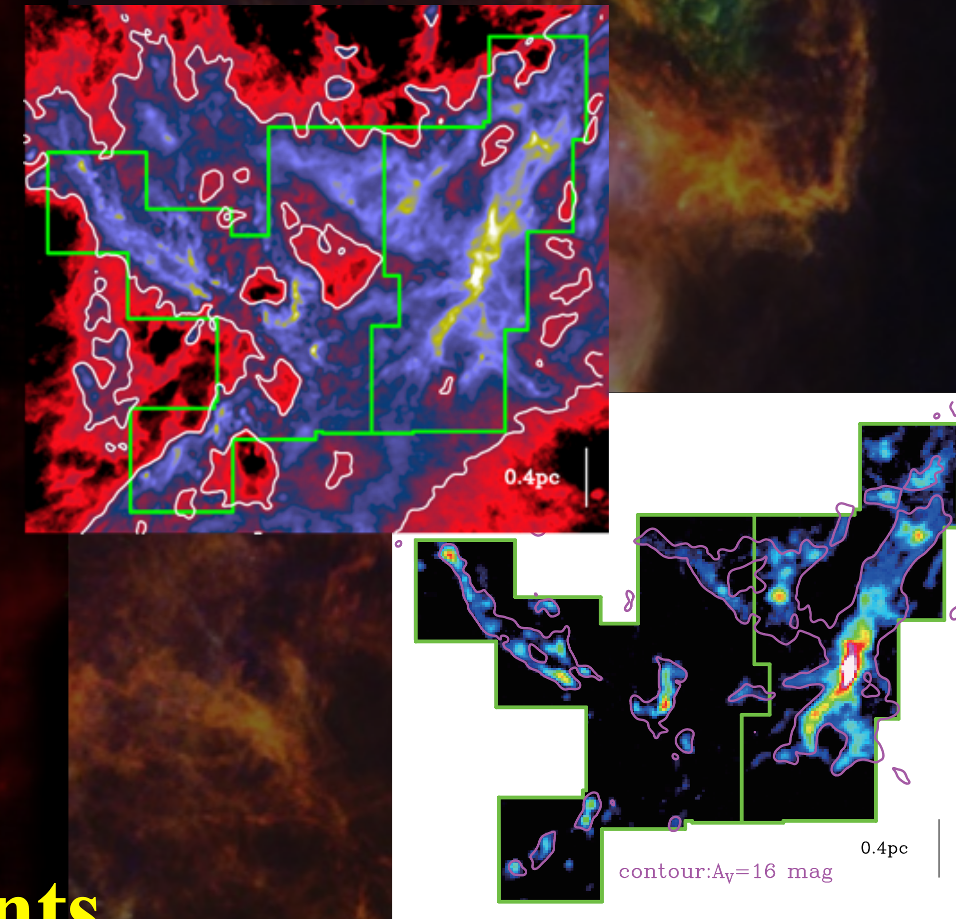


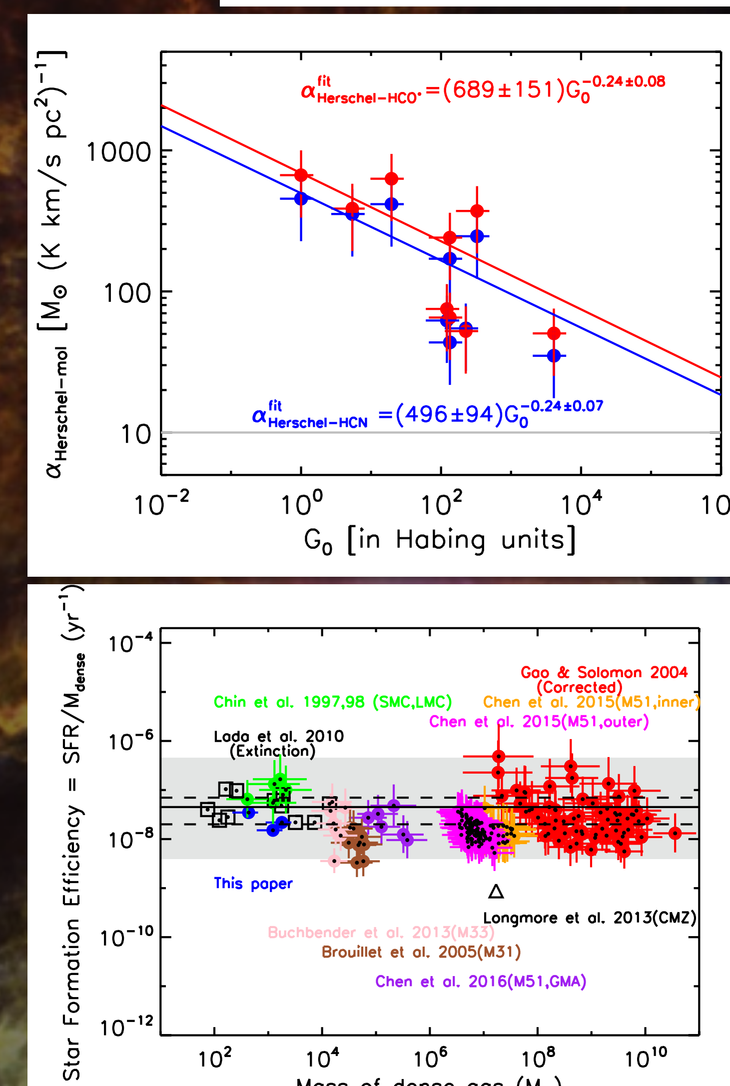

# 南極望遠鏡によるHCN観測

## HCH(1-0) — optically thick

●Obs. in higher-J HCN or its isotope toward nearby clouds and etragal.

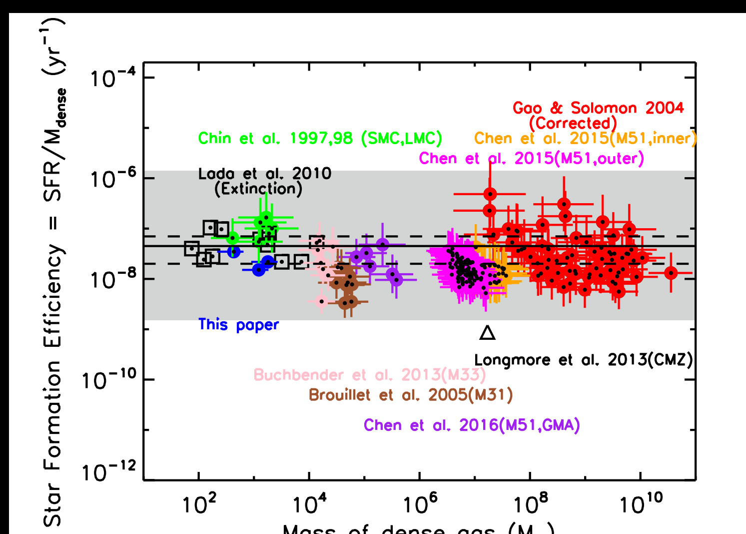


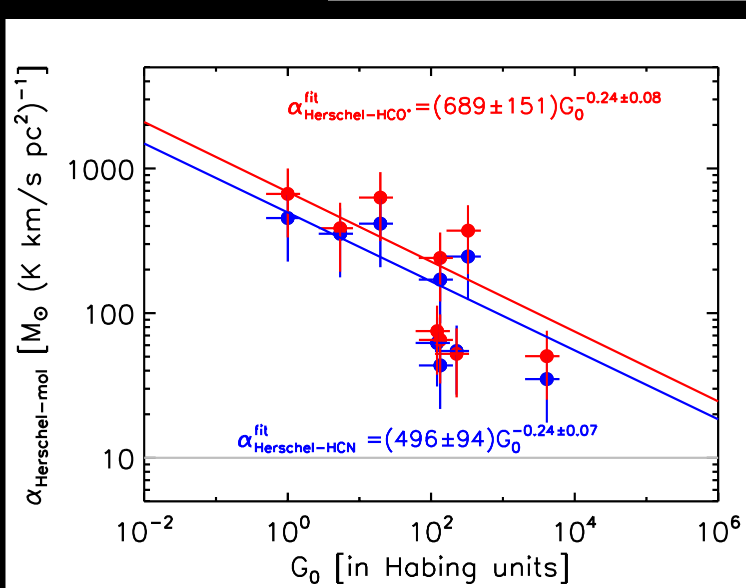


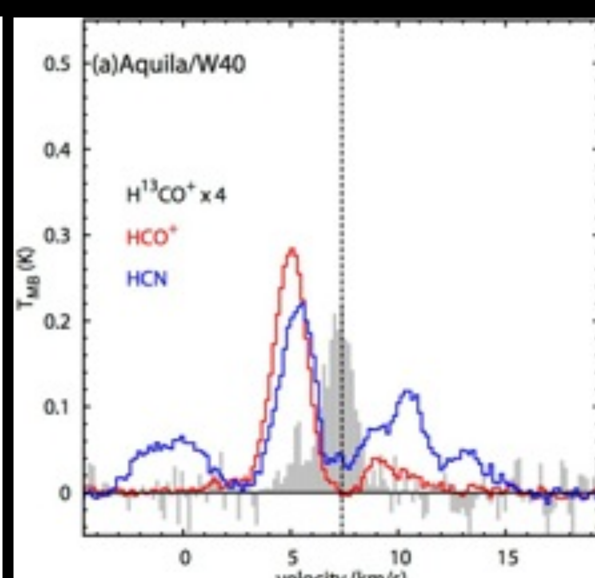


## Contamination from lower Av area

●Wide field mapping toward nearby clouds to evaluate the contamination.

●Obs. in continuum are also required to estimate $M_{dense}$.

HGBS $N(H_2)$

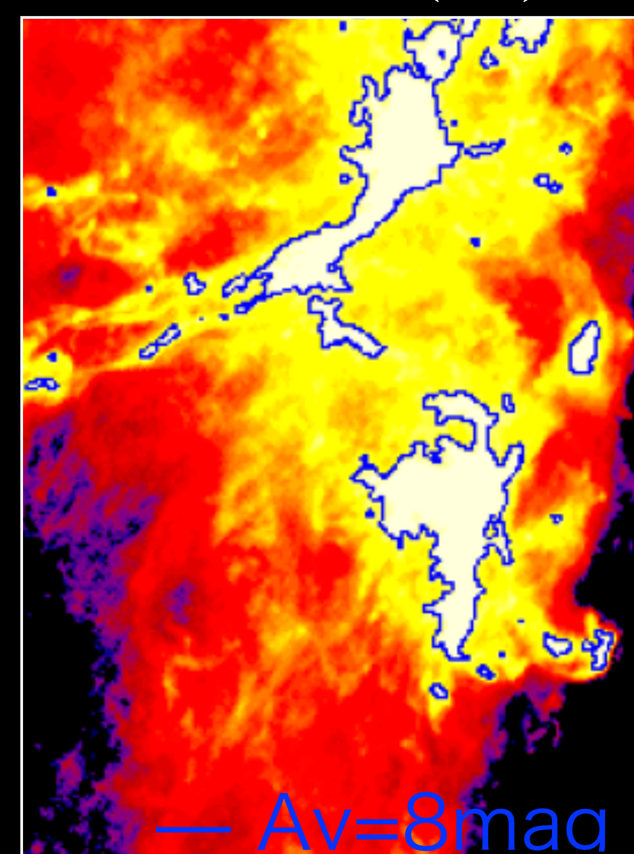


HCN(1-0)

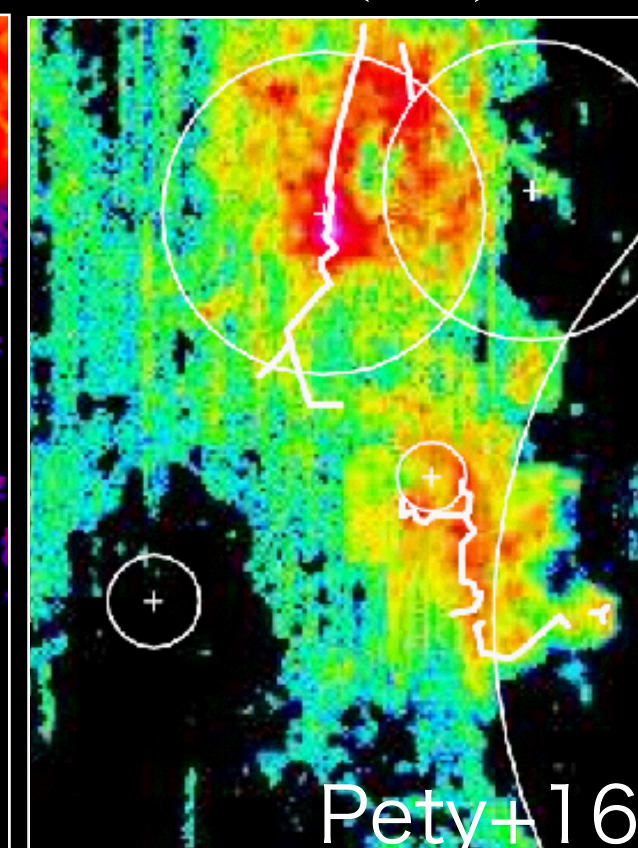

# 南極望遠鏡による連続波観測



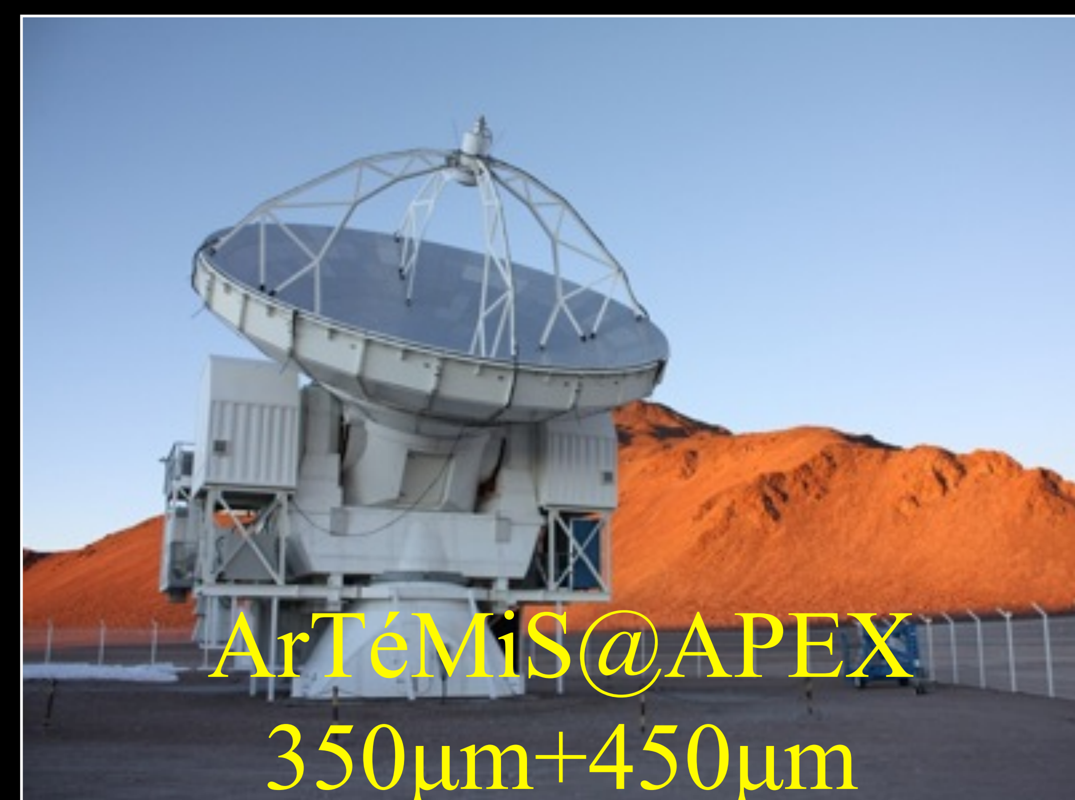

# 南極望遠鏡による連続波観測

AzTEC/ASTE

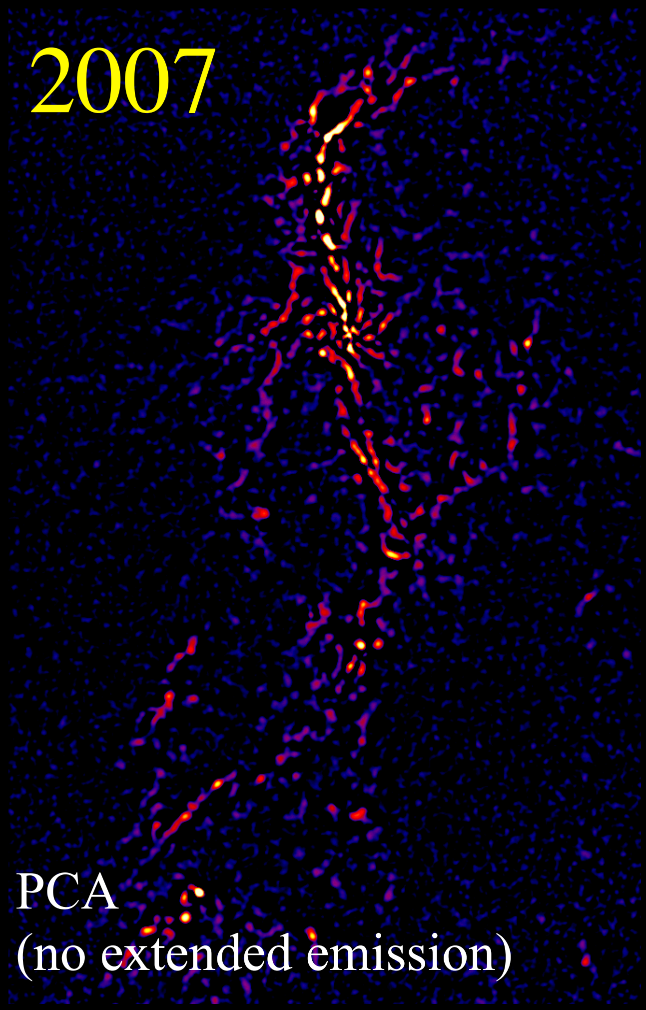


Shimajiri et al. 2011,2015a

Intensity profiles around strong sources

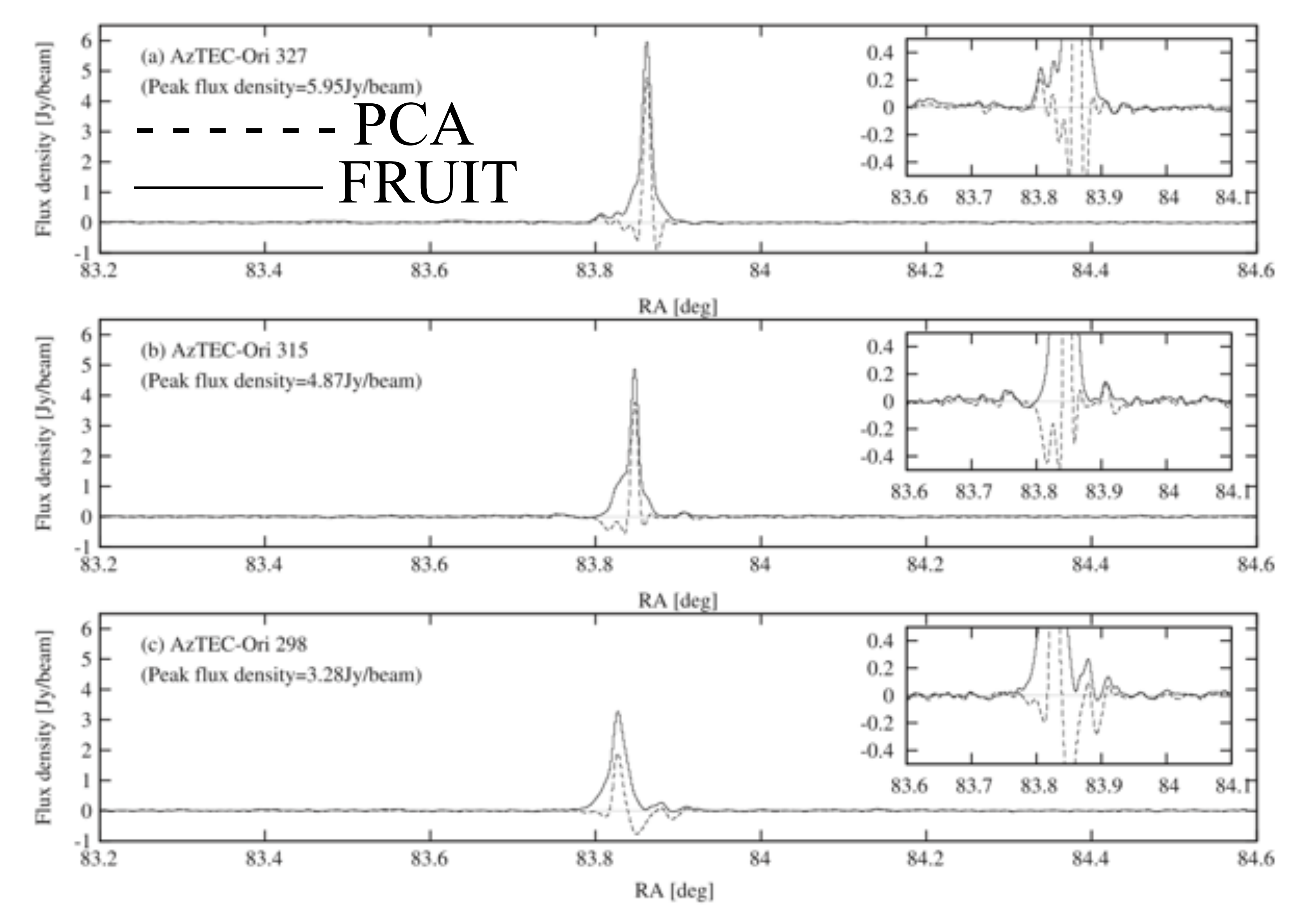

# 南極望遠鏡による連続波観測

AzTEC/ASTE

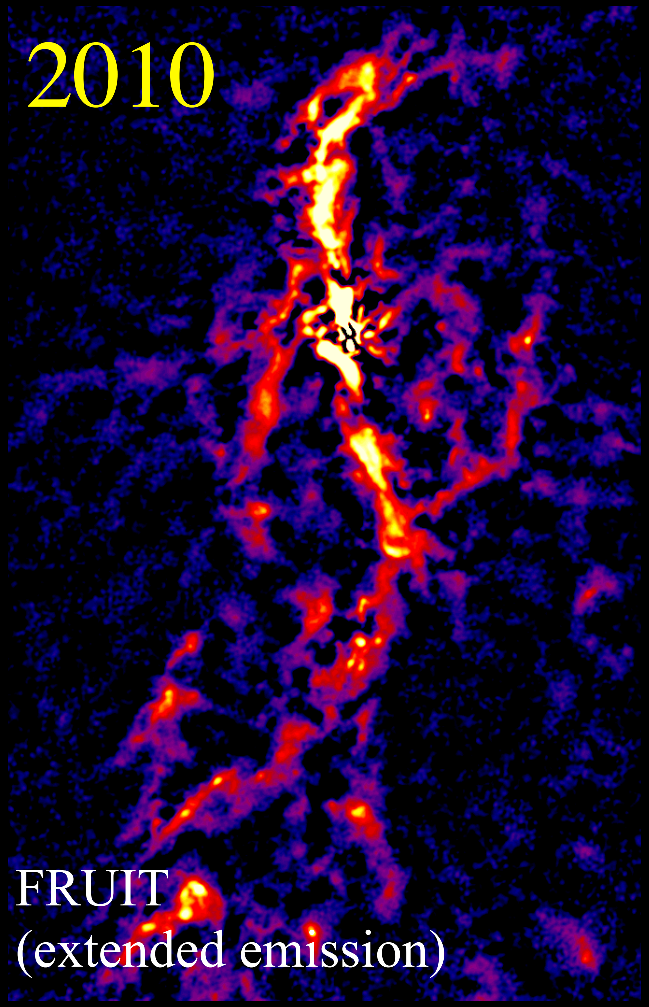


Shimajiri et al. 2011,2015a

Intensity profiles around strong sources

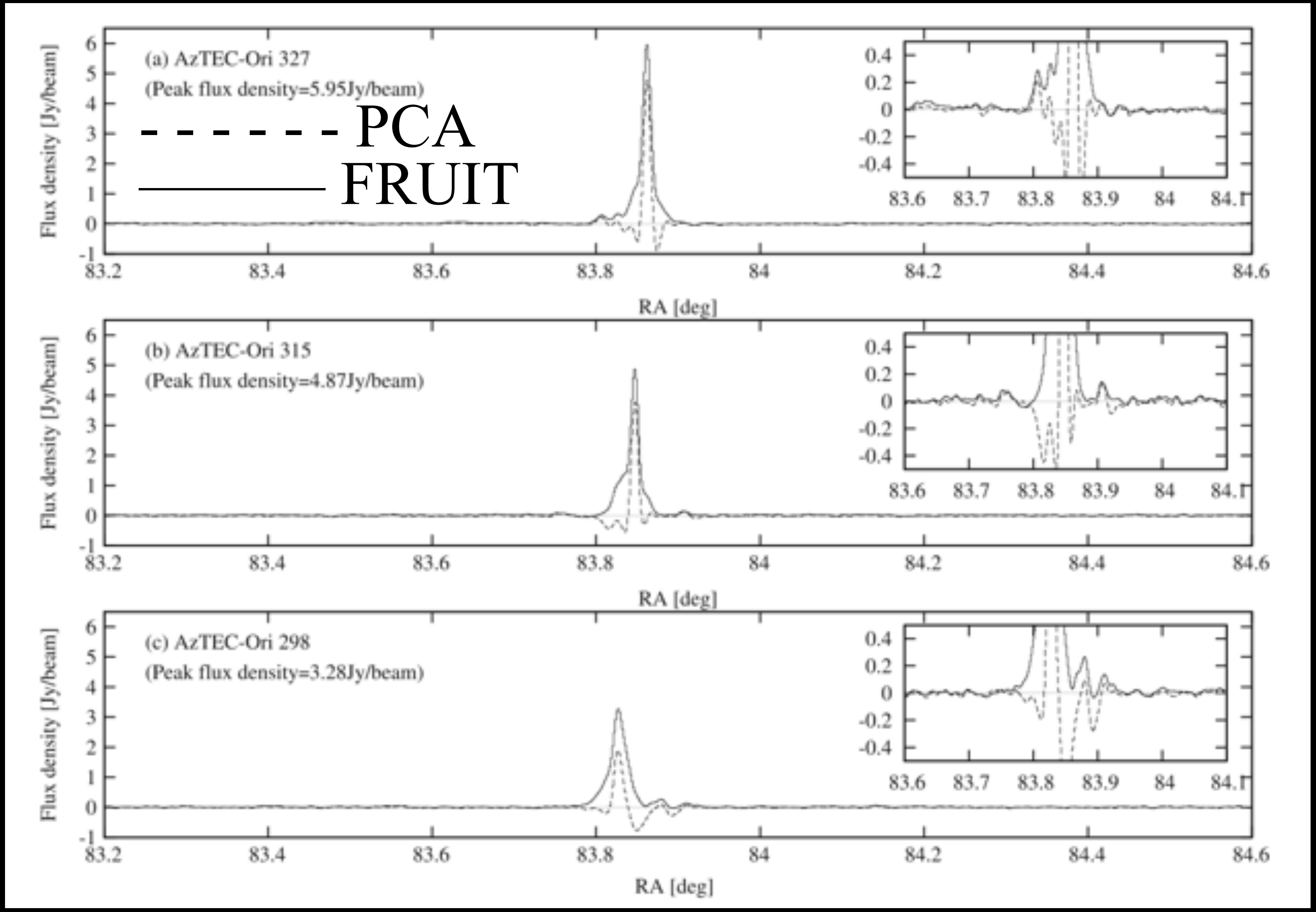


Reconstructing extended emission is crucial
for star formation studies

# 南極望遠鏡による連続波観測

ArTeMiS/APEX

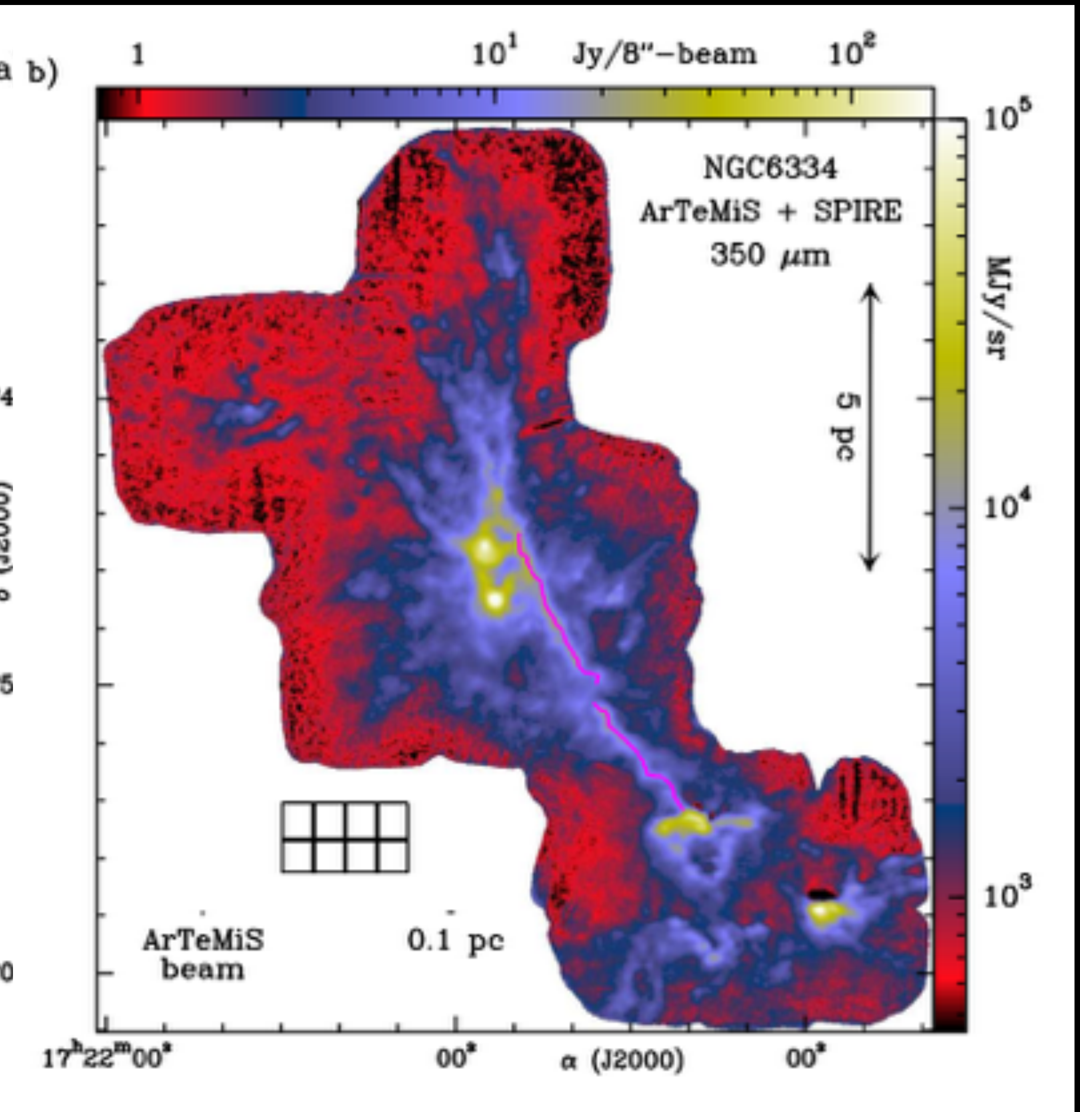


Andre et al. 2016

ESO news letter (14 Junes 2016)

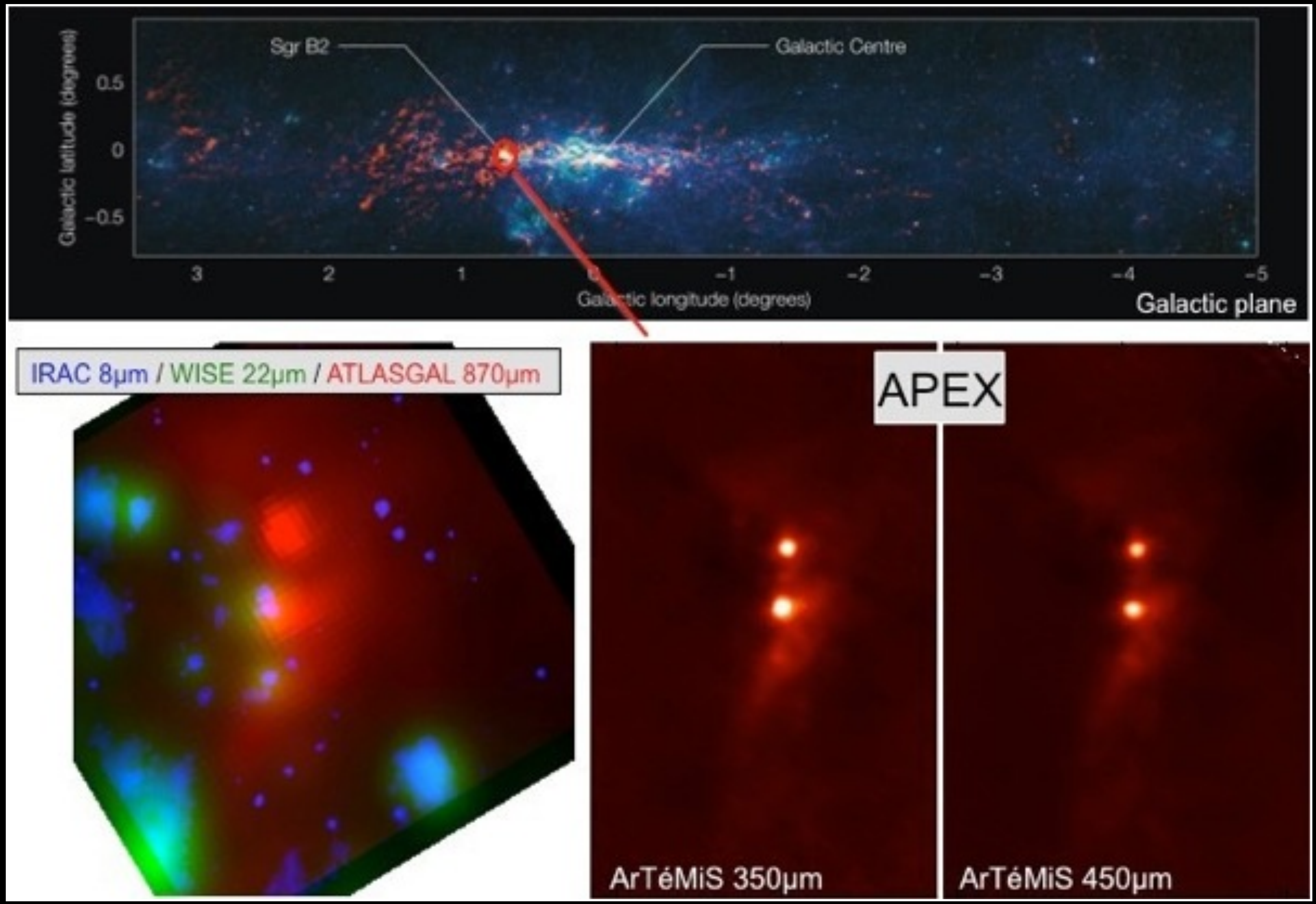


http://www.eso.org/sci/publications/announcements/sciann16034.html

Combined APEX/ArTeMiS image with Herschel/SPIRE image.

*Thank you*

# Dense gas in low-metallicity galaxies

J. Braine[1], Y. Shimajiri[2], P. André[2], S. Bontemps[1], Yu Gao[3,4], Hao Chen[5,6,7], and C. Kramer[8]

[1] Laboratoire d'Astrophysique de Bordeaux, Univ. Bordeaux, CNRS, B18N, alle Geoffroy Saint-Hilaire, 33615 Pessac, France. e-mail: jonathan.braine@u-bordeaux.fr
[2] Laboratoire AIM, CEA/DRF–CNRS–Université Paris Diderot, IRFU/Service dAstrophysique, C.E. Saclay, Orme des Merisiers, 91191 Gif-sur-Yvette, France
[3] Purple Mountain Observatory, Chinese Academy of Sciences, 2 West Beijing Road, Nanjing 210008, P. R. China;
[4] Key Laboratory of Radio Astronomy, Chinese Academy of Sciences, Nanjing 210008, P. R. China
[5] School of Astronomy and Space Science, Nanjing University, Nanjing 210093, P. R. China
[6] Key Laboratory of Modern Astronomy and Astrophysics, Nanjing University, Nanjing 210093, P. R. China
[7] Collaborative Innovation Center of Modern Astronomy and Space Exploration, Nanjing 210093, P. R. China
[8] Instituto Radioastronoma Milimétrica, Av. Divina Pastora 7, Nucleo Central, 18012 Granada, Spain

Received xxxx; accepted xxxx

## ABSTRACT

Stars form out of the densest parts of molecular clouds. Far-IR emission can be used to estimate the Star Formation Rate (SFR) and high dipole moment molecules, typically HCN, trace the dense gas. A strong correlation exists between HCN and Far-IR emission, with the ratio being nearly constant, over a large range of physical scales. A few recent observations have found HCN to be weak with respect to the Far-IR and CO in subsolar metallicity (low-Z) objects. We present observations of the Local Group galaxies M 33, IC 10, and NGC 6822 with the IRAM 30meter and NRO 45m telescopes, greatly improving the sample of low-Z galaxies observed. HCN, $HCO^+$, CS, $C_2H$, and HNC have been detected. Compared to solar metallicity galaxies, the Nitrogen-bearing species are weak (HCN, HNC) or not detected (CN, HNCO, $N_2H^+$) relative to Far-IR or CO emission. $HCO^+$ and $C_2H$ emission is normal with respect to CO and Far-IR. While $^{13}CO$ is the usual factor 10 weaker than $^{12}CO$, $C^{18}O$ emission was not detected down to very low levels. Including earlier data, we find that the HCN/$HCO^+$ ratio varies with metallicity (O/H) and attribute this to the sharply decreasing Nitrogen abundance. The dense gas fraction, traced by the HCN/CO and $HCO^+$/CO ratios, follows the SFR but in the low-Z objects the $HCO^+$ is much easier to measure. Combined with larger and smaller scale measurements, the $HCO^+$ line appears to be an excellent tracer of dense gas and varies linearly with the SFR for both low and high metallicities.

**Key words.** Galaxies: Individual: M 33 – Galaxies: Individual: IC 10 – Galaxies: Individual: NGC 6822 – Galaxies: Local Group – Galaxies: ISM – Stars: Formation

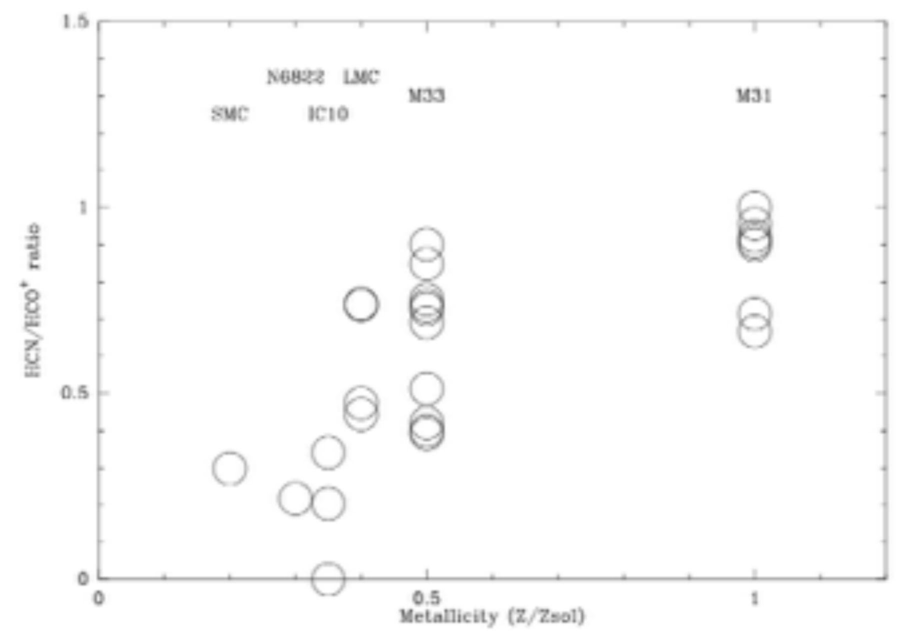


**Fig. 8.** Variation of the HCN/$HCO^+$ ratio with metallicity. References are Brouillet et al. (2005); Chin et al. (1997, 1998) for M 31 and the Magellanic Clouds, Buchbender et al. (2013) and the present work for M 33, and this work for IC 10 and NGC 6822. Typical uncertainties for individual points are 0.2 dex for the metallicity and 0.3 in the HCN/$HCO^+$ ratio.